Yan Jing, Wen-chun Ge, Hao Yang, Yu Dong, Zheng Ji, Jun-hui Bi, Hong-ying Zhou, and De-he Xing, 2022, High-magnesium igneous associations record final-stage geodynamic process of the southeastern segment of the Central Asian Orogenic Belt: GSA Bulletin, https://doi.org/10.1130/B36472.1.

Supplemental Material

Text. Methods and References for Table S5.

Figure S1. Diagrams showing chondrite-normalized REEs patterns for zircons from the high-Mg igneous associations in the Qinghe region.

Figure S2. Diagrams showing variation of selected elements vs. LOI to check for element mobility during post-magmatic alteration.

Figure S3. (A) SiO_2 vs. Th/La and (B) MgO vs. Nb/La diagrams of the high-Mg igneous rocks in the Qinghe region.

Figure S4. (A) MgO vs. CaO; (B) MgO vs. Cr; (C) MgO vs. Ni; (D) MgO vs. TiO_2; (E) Sr vs. Ba; and (F) TiO_2 versus V diagrams of the high-Mg igneous rocks in the Qinghe region. Mineral abbreviations: Ol—olivine; Hbl—hornblende; Cpx—clinopyroxene; Pl—plagioclase; Kf—potassium feldspar; Bi—biotite.

Figure S5. Diagrams of (A) Nb/Yb vs. Th/Yb; (B) Th/Yb vs. La/Yb of the high-Mg igneous rocks in the Qinghe region.

Table S1. LA-ICP-MS and SIMS zircon U-Pb data of the Triassic high-magnesium igneous associations in the southeastern segment of the CAOB.

Table S2. Major (wt%) and trace (ppm) elements of the Triassic high-magnesium igneous associations in the southeastern segment of the CAOB.

Table S3. In situ zircon Hf isotopic compositions of the Triassic high-magnesium igneous associations in the southeastern segment of the CAOB. The red font in Table S3 represents the zircon Hf isotopic results of inherited zircons.

Table S4. Zircon O isotopic compositions of the standard samples and Early Triassic high-magnesium andesites in the southeastern segment of the CAOB. The red font in Table S4 represents the zircon O isotopic results of inherited zircons.

Table S5. Reported geochronological data for the Late Paleozoic-Early Mesozoic magmatic rocks along the Solonker-Xar Moron-Changchun-Yanji suture zone. Associated references are presented in Supporting data.

Supporting Information for

High-magnesium igneous associations record final-stage geodynamic process of the southeastern segment of the Central Asian Orogenic Belt

Yan Jing [1,2], Wen-chun Ge [1,2*], Yu Dong [1,2], Hao Yang [1,2], Zheng Ji [1,2], Jun-hui Bi [1,2], Hong-ying Zhou [3], De-he Xing [4]

[1] College of Earth Sciences, Jilin University, Changchun 130061, China

[2] Key Laboratory of Mineral Resources Evaluation in Northeast Asia, Ministry of Land and Resources of China, Changchun 130026, China

[3] Tianjin Center, China Geological Survey, Tianjin 300170, China

[4] Shenyang Center, China Geological Survey, Shenyang 110034, China

Contents of this file

Introduction

This supplementary material provided additional information on:

1. Methods

1.1. Zircon U-Pb dating

Zircon crystals were extracted from whole-rock samples by combining magnetic with heavy liquid separation techniques, and then by handpicking under a binocular microscope at the Langfang Regional Geological Survey, Hebei Province, China. These zircons were then examined under transmitted and reflected light micrographs with an optical microscope, and imaged using CL. The CL images were used to characterize the internal textures and choose potential targets for U-Pb dating and Hf-O analyses, such as the transparent, euhedral, unfractured, and inclusion-free zircons. CL images were collected using a CL spectrometer (Garton Mono CL3+) equipped on a Quanta 200F Scanning Electron Microscope with a 2 min scan time at conditions of 15 kV and 120 nA at Peking University.

Zircon U-Pb dating for sample (18FK020) was measured using a secondary ion mass spectrometry (SIMS) at the Institute of Geology and Geophysics, Chinese Academy of Sciences (IGGCAS) in Beijing. SIMS zircon U-Pb analyses were conducted utilizing a Cameca IMS 1280 icon microprobe. The SIMS methodology adopted during the analytical process follows analytical descriptions described by Li et al. (2009). The resulted ellipsoidal spot is about 20 × 30 μm in size. To monitor the external uncertainties of SIMS U-Pb measurements, analyses of zircon standard Qinghu were interspersed with unknowns. Twenty-four analyses during this analytical process yielded a weighted mean $^{206}Pb/^{238}U$ age of 159.6 ± 1.6 Ma (MSWD = 0.003, 96% confidence interval), identical within errors to the reported age of 159.5 ± 0.2 Ma (Li et al., 2013).

Zircon U-Pb dating and trace element analyses for samples (18KY001 and 18KY006) were conducted using a LA-ICP-MS at the Institute of Geology and Mineral Resources in Tianjin, China. In the analytical process, the spot size for data collection was 32 μm, with an energy density of 10 J/cm^2 and repetition rate of 8 Hz. The zircon standards 91500 and GJ were used to calibrate the U-Th-Pb ratios. The errors for individual U-Pb analyses are presented with 1σ error and uncertainties in grouped ages are quoted at 95% level (1σ). Off-line inspection and intergration of background and analysis signals, and time-drift correction and quantitative calibration for trace element analyses and U-Pb dating were performed using ICP-MS DataCal (Liu et al., 2010). Further detailed descriptions of the instrumentation and analytical procedure for the LA-ICP-MS zircon U-Pb and trace element technique are similar to those described by Yuan et al. (2004).

The zircon U-Pb analyses for other samples were performed using an Agilent 7500a inductively coupled plasma mass spectrometer (ICP-MS) equipped with a 193 nm ArF Excimer laser system (LA), housed at Key Laboratory of Mineral Resources Evaluation in Northeast Asia, Ministry of Land and Resources of China. The spot size was 32 μm, with an energy density of 10 J/cm^2 and repetition rate of 8 Hz. Zircon 91500 was used as the external standard for age calibration and the standard silicate NIST 610 glass was used to optimize concentration calculations (Wiedenbeck et al., 1995). Zircon standard Plesovice (337 Ma) was used to supervise any deviation of age measurement. Isotopic ratios and element concentrations were calculated using Glitter program (ver.4.4, Macquarie University). The age calculation and concordia plots were obtained using Isoplot (ver 3.0) (Ludwig, 2003). The common Pb was corrected using the method of Andersen (2002).

1.2. Major and trace elements analyses

Bulk rock major and trace elements analyses for samples (17FK09 and 17FK10) were performed at the Geological Lab Center of China University of Geosciences, Beijing (CUGB). Bulk-rock major element oxides were determined using inductively coupled plasma-atomic emission spectroscopy (ICP-OES). The analytical precisions (1σ) are generally <1% for most elements with the exception of TiO_2 (~1.5%) and P_2O_5 (~2.0%) based on rock standards GRS-1, and GSR-3 (national geological standard reference material of China), AGV-2, W-2 (US Geological Survey). Loss on ignition (LOI) was determined by placing 1 g of samples in the furnace at 1000 °C for several hours before being cooled in a desiccator and reweighed. The trace element analyses were determined on an Agilent-7500a ICP-MS at the Institute of Earth Science, CUGB. Rock standards AGV-2, W-2, and BHVO-2 (US Geological Survey) were used to monitor the analytical accuracy and precision. Analytical accuracy, as indicated by relative difference between measured and recommended values, is better than 5% for most elements, and better than 10–15% Ta and Gd. The detailed analytical procedures follow Song et al. (2010).

Whole-rock major and trace elements geochemical analyses for other samples were conducted at Wuhan SampleSolution Analytical Technology Co., Ltd., Wuhan, China. Major element concentrations were determined by a Rigaku-3080 X-ray fluorescence (XRF) employing a Rh-anode X-ray tube with a voltage of 40 kV and a current of 70 mA after samples were fused in a high-frequency melting furnace. The analytical precision (relative standard deviation, RSD) and accuracy (relative error, RE) are both better than 4% for the major element concentrations determined during this study, and further details of the analytical procedures used are given in Ma et al. (2012). Trace element compositions were determined by ICP-MS employing Agilent

7500a and Elan 6100 DRC instruments after the acid digestion of samples in Teflon bombs, with analytical accuracy better than 5% for most elements. Sample digestion procedures and the resulting analytical precision and accuracy are reported in Liu et al. (2008).

1.3. *In situ* zircon Hf isotopic analyses

In situ zircon Hf isotopic analyses were undertaken using a Neptune multi-collector (MC) ICP-MS, equipped with a 193 nm ArF Excimer laser system at the Tianjin Institute of Geology and Mineral Resources in Tianjin, China. Instrument settings and a detailed outline of analytical procedures are illustrated by Wu et al. (2006) and Geng et al. (2011). The Lu-Hf isotopic analyses were performed on the same zircon crystals that were previously used for U-Pb isotopic analyses, with a spot diameter of 50 μm, an ablation time of 23 s, and an ablation rate of 8 Hz. The international standard zircon 91500 (Harvard University) was used to monitor the instrument and correct for external parts of samples. Measured $^{176}Hf/^{177}Hf$ and $^{176}Lu/^{177}Hf$ ratios were used to calculate the initial $^{176}Lu/^{177}Hf$ ratio according to the decay constant for ^{176}Lu of 1.865×10^{-11} year^{-1}. The present–day chondritic ratios of $^{176}Hf/^{177}Hf$ =0.282772 and $^{176}Lu/^{177}Hf$ = 0.0332 were adopted to calculate $\varepsilon_{Hf}(t)$ values (Blichert and Albarède, 1997). For the calculation of two-stage Hf model ages (T_{DM2}), $^{176}Hf/^{177}Hf$, $^{176}Lu/^{177}Hf$ and fcc were 0.28325, 0.282772 and –0.548, respectively (Blichert and Albarède., 1997; Veevers et al., 2005). Details of the analytical procedures are described by Wu et al. (2006).

1.4. *Z*ircon oxygen isotopic analyses

Zircon oxygen isotopes of basaltic rock samples were measured using the Cameca IMS-1280 SIMS at the IGGCAS in Beijing. The detailed analytical procedures were similar to those described in Li et al. (2010a). The measured oxygen isotopic data were corrected for instrumental mass fractionation (IMF) using the Penglai zircon standard (δO_{VSMOW} = 5.3‰; Li et al., 2010b). The internal precision of a single analysis generally was better than 0.2‰ (1σ) for the $^{18}O/^{16}O$ ratio. The external precision, measured by the reproducibility of repeated analyses of Penglai standard, is 0.41‰ (2σ, n = 120). Measurements of the Qinghu zircon standard during the course of this study yielded a weighted mean of $^{\delta}18O$ = 5.3 ± 0.6‰ (2σ), which is consistent within errors with the reported value of 5.3 ± 0.3‰ (Li et al., 2013).

References

Andersen, T., 2002, Correction of common lead in U-Pb analyses that do not report ^{204}Pb: Chemical Geology, v. 192, no. 1, p. 59–79.

Blichert-Toft, J., & Albarède, F., 1997, The Lu-Hf isotope geochemistry of chondrites and the evolution of the mantle-crust system: Earth and Planetary Science Letters, v. 148, no. 1, p. 243–258.

Geng J.Z., Li H.K., Zhang, J., Zhou, H.Y., & Li, H.M.. 2011, Zircon Hf isotope analysis by means of LA-MC-ICP-MS: Geological Bulletin of China, v. 10, p. 1508–1513 (in Chinese with English abstract).

Li, X. H., et al., 2010b, Penglai zircon megacrysts: A potential new working reference material for microbeam determination of Hf-O isotopes and U-Pb age: Geostandards and Geoanalytical Research, v. 34, no. 2, p. 117–134.

Li, X. H., Li, W.X., Li, Q. L. Wang, X.C,. Liu, Y., & Yang, Y.H., 2010a, Petrogenesis and tectonic significance of the ~850 Ma Gangbian alkaline in South China: Evidence from in situ zircon U-Pb dating, Hf-O isotopes and whole-rock geochemistry: Lithos, v. 114, no. 1–2, p. 1–15.

Li, X.H., Liu, Y., Li, Q.L., Guo, C.H., & Chamberlain, K.R., 2009, Precise determination of Phanerozoic zircon Pb/Pb age by multicollector SIMS without external standardization: Geochemistry, Geophysics, Geosystems, v. 10, p. 1–21.

Li, X.H., Tang, G.Q., Gong, B., Yang, Y.H., Hou, K.J., Hu, Z.C., et al., 2013, Qinghu zircon: a working reference for microbeam analysis of U-Pb age and Hf and O isotopes: Chinese Science Bulletin, v. 58, p. 4647–4654.

Liu, Y.S., Hu, Z.C., Zong, K.Q., Gao, C.G., Gao, S., Xu, J., & Chen, H.H., 2010, Reappraisement and refinement of zircon U-Pb isotope and trace element analyses by LA-ICP-MS. Chinese Science Bulletin, v. 55, p. 1535–1546.

Liu, Y.S., Zong, K.Q., Kelemen, P.B., & Gao, S., 2008, Geochemistry and magmatic history of eclogites and ultramafic rocks from the Chinese continental scientific drill hole: subduction and ultrahigh-pressure metamorphism of lower crustal cumulates: Chemical Geology, v. 247, p. 133–153.

Ludwig, K.R., 2003, User's Manual for Isoplot 3.0: A Geochronological Toolkit for Microsoft Excel. vol. 4: Berkeley Geochronology Center, p. 1–71 (special publication).

Ma, Q., Zheng, J.P., Griffin, W.L., Zhang, M., Tang, H.Y., Su, Y.P., & Ping, X.Q., 2012, Triassic “adakitic” rocks in an extensional setting (North China): melts from the cratonic lower crust: Lithos, v. 149, p. 159–173.

Song, S.G., Niu, Y.L., Wei, C.J., Ji, J.Q., & Su, L., 2010, Metamorphism, anatexis, zircon ages and tectonic evolution of the Gongshan block in the northern Indochina continent-an eastern extension of the Lhasa Block: Lithos, v. 120, p. 327–346.

Veevers, J.J., Saeed, A., Belousova, E.A., Griffin, & W.L., 2005, U-Pb ages and source composition by Hf-isotope and trace-element analysis of detrital zircons in Permian sandstone and modern sand from southwestern Australia and a review of the paleogeographical and denudational history of the Yilgarn Craton: Earth-Science Reviews, v. 68, no. 3, p. 245–279.

Wiedenbeck, M., Alle, P., Corfu, F., Griffin, W.L., Meier, M., Oberli, F., Vonquadt, A., Roddick, J.C., & Speigel, W., 1995, Three natural zircon standards for U-Th-Pb, Lu-Hf, trace-element and REE analyses: Geostandards and Geoanalytical Research, v. 19, no. 1, p. 1–23.

Wu, F.Y., Yang, Y.H., Xie, L.W., Yang, J.H., & Xu, P., 2006, Hf isotopic compositions of the standard zircons in U-Pb geochronology: Chemical Geology, v. 234, p. 105–126.

Yuan, H.L., Gao, S., Liu, X.M., Li, H.M., Günther, D., & Wu, F.Y., 2004, Accurate U–Pb age and trace element determinations of zircon by Laser Ablation-Inductively Coupled Plasma-Mass Spectrometry: Geostandards and Geoanalytical Research, v. 28, p. 353–370.

2. References for Table.S5

Cao, H.H., Xu, W.L., Pei, F.P., Guo, P.Y., & Wang, F., 2012, Permian tectonic evolution of the eastern section of the northern margin of the North China Plate: constraints from zircon U-Pb geochronology and geochemistry of the volcanic rocks: Acta Petrologica Sinica, v. 28, p. 2733–2750 (in Chinese with English abstract).

Cao, H.H., Xu, W.L., Pei, F.P., Wang, Z.W., Wang, F., & Wang, Z.J., 2013, Zircon U-Pb geochronology and petrogenesis of the Late Paleozoic-Early Mesozoic intrusive rocks in the eastern segment of the northern margin of the North China Block: Lithos, v. 170, p. 191–207.

Cao, H.H., Xu, W.L., Pei, F.P., & Zhang, X.Z., 2011, Permian tectonic evolution in Southwestern Khanka massif: evidence from zircon U-Pb chronology, Hf isotope and geochemistry of gabbro and diorite: Acta Geologica Sinica (English Edition), v. 85, p. 1390–1402.

Chen, Y.J., Pen G.Y.J., Liu, Y.W., Sun, G., & G.M., 2006, Progress in the Study of Chronostratigraphy of the"Qinghezhen Group": Geological Review, v. 2, p. 170–177 (in Chinese with English abstract).

Fu, C.L., Sun, D.Y., Zhang, X.Z.,Wei, H.Y., & Gou, J., 2010, Discovery and geological significance of the Triassic high-Mg diorites in Hunchu area, Jilin Province: Acta Petrologica Sinica, v. 26, no. 4, p. 1089–1102 (in Chinese with English abstract).

Gu, C.C., Zhu, G., Li, Y.J., Su, N., Xiao, S.Y., Zhang, S., & Liu, C., 2018, Timing of deformation and location of the eastern Liaoyuan Terrane, NE China: Constraints on the final closure time of the Paleo-Asian Ocean: Gondwana Research, v. 60, p. 194–212.

Gu, C.C., Zhu, G., Zhai, M.J., Lin, S.Z., Song, L.H., & Liu, B., 2016, Features and origin time of Mesozoic strike-slip structures in the Yilan-Yitong Fault zone: Science China Earth Sciences, v. 59, p. 2389–2410.

Guan, Q.B., Li, S.C., Zhang, C.; Shi, Y., & Li P.C., 2016, Zircon U-Pb dating, geochemistry and geological significance of the I-type granites in Helong area, the eastern section of the southern margin of Xing-Meng Orogenic Belt: Acta Petrologica Sinica, v. 32, p. 2690–2706 (in Chinese with English abstract).

Guo, F., Li, H.X., Fan, W.M., Li, J.Y., Zhao, L., & Huang, M.W., 2016, Variable sediment flux in generation of Permian subduction-related mafic intrusions from the Yanbian region, NE China: Lithos, v. 261, p. 195–215.

Li, C.D., Zhang, F.Q., Miao, L.C., Xie, H.Q., & Xu, Y.W., 2007, Zircon SHRIMP geochemistry of late Permian high-Mg andesites in Seluohe area, Jilin Province, China: Acta Petrologica Sinica, v. 23, p. 767–776 (in Chinese with English abstract).

(LBGMR) Liaoning Bureau of Geology and Mineral Resources, 1998, 1:50000 scale regional geology of the Diaobingshan, Wutaizi, and Daming, Liaoning Province (in Chinese).

Liu, J., Liu, Z.H., Li, S.C., Zhao, C., Wang, C.J., Peng, Y.B., Yang, Z.J., & Dou, S.Y., 2016a, Geochronology and geochemistry of Triassic intrusive rocks in Kaiyuan area of the eastern section of the northern margin of North China: Acta Petrologica Sinica, v. 32, p. 2739–2756 (in Chinese with English abstract).

Liu, J., Yang, Z.Z., Chen, S.L., Zhang, L.Z., Li, H.M., Chen, C., & Yang, L., 2016b, Zircon SHRIMP age of the stratified metamorphic rocks in Faku area, northern Liaoning Province: geological implication: Geology and Resources, v. 25, p. 22–25 (in Chinese with English abstract).

Liu, J., Zhang, J., Liu, Z.H., Yin, C.Q., Zhao, C., Yu, X.Y., Tian,Y., & Dong, Y., 2020, Petrogenesis of Permo–Triassic intrusive rocks in Northern Liaoning Province, NE China: implications for the closure of the eastern Paleo-Asian Ocean: International Geology Review, 62, no. 6, 754–780.

Liu, S., Hu, R.Z., Gao, S., Feng, C.X., Feng, G.Y., Coulson, I.M., Li, C., Wang, T., & Qi, Y.Q., 2010, Zircon U-Pb age and Sr-Nd-Hf isotope geochemistry of Permian granodiorite and associated gabbro in the Songliao Block, NE China and implications for growth of juvenile crust: Lithos, v. 114, p. 423–436.

Ma, X.H., Chen, C.J., Zhao, J.X., Qiao, S.L., & Zhou, Z.H., 2019, Late Permian intermediate and felsic intrusions in the eastern Central Asian Orogenic Belt: Final-stage magmatic record of Paleo-Asian Oceanic subduction: Lithos, v. 326–327, p. 265–278.

Pei, F.P., Zhang, Y., Wang, Z.W., Cao, H.H., Xu, W.L., Wang, F., & Yang, C., 2016, Early–Middle Paleozoic subduction–collision history of the south-eastern Central Asian Orogenic Belt: Evidence from igneous and metasedimentary rocks of central Jilin Province, NE China: Lithos, v. 261, p. 164–180.

Shi, Y., Liu, Z.H., Xu, Z.Y., Wang, X.A., Zhang, C., Liu, W.Z., & Chen, X., 2013, Isotopic chronology and geochemistry of the hercynian Yongxin granitoid in Longjing, Jilin Province: Geology and Resources, v. 1, p. 6–13 (in Chinese with English abstract).

Song, Z.G., Han, Z.Z., Gao, L.H., Geng, H.Y., Li, X.P., Meng, F.X., Han, M., Zhong, W.J., Li, J.J., Du, Q.X., Yan, J.L., & Liu, H., 2018, Permo-Triassic evolution of the southern margin of the Central Asian Orogenic Belt revisited: Insights from Late Permian igneous suite in the Daheishan Horst, NE China: Gondwana research, v. 56, p. 23–50.

Sun, D.Y., Wu, F.Y., Zhang, Y.B., & Gao, S., 2004, The final closing time of Xiramuron-Changchun-Yanji plate suture zone: evidence from the Dayushan granitic pluton of Jilin: Journal of Jilin University (Earth Science Edition), v. 34, p. 174–181 (in Chinese with English abstract).

Sun, D.Y., Wu, F.Y., Gao, S., & Lu, X.P., 2005, Confirmation of two episodes of A-type granite emplacement during Late Triassic and Early Jurassic in the central Jilin Province, and their constraints on the structural pattern of the east Jilin-Heilongjiang area, China (in Chinese with English abstract): Earth Science Frontiers, v. 12, no. 2, p. 263–275.

Wang, Z.J., Xu, W.L., Pei, F.P., & Cao, H.H., 2013a, Middle Permian-Early Triassic mafic magmatism and its tectonic implication in the eastern section of the southern margin of the Xing'an-Mongolian Orogenic Belt, NE China: Constraints from zircon U-Pb geochronology and geochemistry: Geological Bulletin of China, v. 32, p. 374–387 (in Chinese with English abstract).

Wang, Z.J., Xu, W.L., Pei, F.P., Wang, Z.W., Li, Y., & Cao, H.H., 2015, Geochronology and geochemistry of middle Permian-Middle Triassic intrusive rocks from central-eastern Jilin Province, NE China: Constraints on the tectonic evolution of the eastern segment of the Paleo-Asian Ocean: Lithos, v. 238, p. 13–25.

Wang, Z.W., Pei, F.P., Cao, H.H., Wang, Z.J., & Xu, W.L., 2013b, Earliest Carboniferous magmatic event in the eastern section of the northern margin of the North China plate and its tectonic implications-Evidence from rock association and zircon U-Pb geochronology: Geological Bulletin of China, v. 32, p. 279–286 (in Chinese with English abstract).

Yang, D.G., Sun, D.Y., Gou, J., & Hou, X.G., 2017, U-Pb ages of zircons from Mesozoic intrusive rocks in the Yanbian area, Jilin Province, NE China: Transition of the Paleo-Asian oceanic regime to the circum-Pacific tectonic regime: Journal of Asian Earth Sciences, v. 143, p. 171–190.

Yu, J.J., Men, L.J., Chen, L., Zhao, J.K., Liang, S.N., Chen, D., & Pang, W., 2008, SHRIMP zircon U-Pb ages and its geological implications from metamorphic dacite of Wudaogou Group in Yanbian area: Journal of Jilin University (Earth Science Edition), v. 38, p. 363–367 (in Chinese with English abstract).

Yu, Q., Ge, W.C., Yang, H., Zhao, G.C., Zhang, Y.L., & Su, L., 2014, Petrogenesis of late Paleozoic volcanic rocks from the Daheshen Formation in central Jilin Province, NE China, and its tectonic implications: constraints from geochronology, geochemistry and Sr-Nd-Hf isotopes: Lithos, v. 192, p. 116–131.

Yuan, L.L, Zhang, X.H., X. F.H., Lu, Y.H., & Zong, K.Q., 2016, Late Permian high-Mg andesite and basalt association from northern Liaoning, North China: Insights into the final closure of the Paleo-Asian ocean and the orogen-craton boundary: Lithos, v. 258, p. 58–76.

Zhang S.,Wang, Y.B., & Chu, S.X., 2012, Zircon U-Pb ages and Sr-Nd-Hf isotopic composition of the Haigou granitoids at the northeastern margin of North China Craton: Implications for geodynamic setting: Acta Petrologica Sinica, v. 2, p. 544–556 (in Chinese with English abstract).

Zhang, C.Y., Zhang, X.Z., & Qiu, D.M., 2007, Ziron U-Pb isotope age and implation of plagioam phibolite in Qinglongcun Group, Yanbian area: Journal of Jilin University (Earth Science Edition), v. 37, p. 672–677 (in Chinese with English abstract).

Zhang, X.H., Su, W.J., & Wang, H., 2005b, Zircon SHRIMP geochronology of the Faku tectonites in the northern Liaoning province: implications for the northern boundary of the North China Craton: Acta Petrologica Sinica, v. 21, p. 135–142 (in Chinese with English abstract).

Zhang, X.H., Wang, H., & Li, T.S., 2005a, $^{40}Ar/^{39}Ar$ geochronology of the Faku tectonites: implications for the tectonothermal evolution of the Faku block, northern Liaoning: Science in China (series D), v. 48, p. 601–612 (in Chinese with English abstract).

Zhang, X.H., Xue, F.H., Yuan, L.L., & Ma, Y.G., & Wilde, S.A., 2012a, Late Permian appinite-granite complex from northwestern Liaoning, North China Craton: Petrogenesis and tectonic implications: Lithos, v. 155, p. 201–217.

Zhang, X.H., Zhang, H.F., Wilde, S.A., Yang, Y. H., & Chen, H.H., 2010, Late Permian to Early Triassic mafic to felsic intrusive rocks from North Liaoning, North China: petrogenesis and implications for Phanerozoic continental crustal growth: Lithos, v. 117, p. 283–306.

Zhang, X.H., Zhang, H.F., Zhai, M.G., Wilde, S.A., & Xie, L.W., 2009, Geochemistry of middle Triassic gabbros from northern Liaoning, North China: origin and tectonic implications: Geological Magazine, v. 146, p. 540–551.

Zhang, Y.B., Wu, F.Y., Wilde, S.A., Zhai, M.G., Lu, X.P., & Sun, D.Y., 2004, Zircon U-Pb ages and tectonic implications of Early Paleozoic granitoids at Yanbian, Jilin Province, Northeast China: Island Arc, v. 13, p. 484–505.

Wu, F. Y., Sun, D. Y., Ge, W. C., Zhang, Y. B., Grant, M. L., Wilde, S. A., & Jahn, B. M., 2011, Geochronology of the Phanerozoic granitoids in northeastern China: Journal of Asian Earth Sciences, v. 41, no. 1, p. 1–30.

Zhao, Q.Y., Li, C.F., Li, D.C., & Chen, Y.J., 2008, Dating for zircons from gabbro dike of Wudaogou Group in Yanbian area and its geological significance: Global Geology, v. 2, p. 150–155 (in Chinese with English abstract).

Zhou, Z.B., Pei F.P., Wang, Z.W., Cao, H.H., Lu, S.M., Xu, W.L., & Zhou, H., 2018, Geochronology and geological implications of Fangniugou volcanic rocks in Yitong area,central Jilin Province: Global Geology, v. 37, p. 46–55 (in Chinese with English abstract).

Miao, L.C., Qiu, Y.M., Fan, W.M., Zhang, F.Q., & Zhai, M.G., 2005, Geology, geochronology, and tectonic setting of the Jiapigou gold deposits, southern Jilin Province, China: Ore Geology Reviews, v. 26, p. 137–165.

Shi, Y., Chen, J.S., Wei, M.H., Shi, S.S., Zhang, C., Zhang, L.D., & Hao, Y.J., 2020, Evolution of eastern segment of the Paleo-Asian Ocean in the Late Paleozoic: Geochronology and geochemistry constraints of granites in Faku area, North Liaoning, NE China: Acta Petrologica Sinica, v. 36, no. 11, p. 3287–3308.

Zhang, X.H., Yuan, L.L., Xue, F.H., & Zhang, Y.B., 2012b, Contrasting Triassic ferroan granitoids from northwestern Liaoning, North China: magmatic monitor of Mesozoic decratonization and a craton-orogen boundary: Lithos, v. 144, p. 12–23.

Yan, D., Zand, X.Y., Ma, C.S., Zhi, Y.B., & Wang, F.L., 2018, Petrogenesis and tectonic setting of Yongxin monzogranite in Helong area, Jilin Province: Global Geology, v. 3, p. 724–736.

Qi, C.D., Ji, C.H., Han, J., & Nie, L.J., 2003, The geologic features of the late Triassic alkali-meta-alkali intrusive complex body of the Dunhua area, Jilin Province and its structural setting: Jilin Geology, v. 22, no. 3, p. 12–18.

Shi, Y., Shi, S.S., Liu, Z.H., Wang, L., Liu, J., Chen, J.S., Yang, F., Zhang, C., Li, B., & Zhang, L.D., 2021, Back-arc system formation and extinction in the southern Central Asian Orogenic Belt: New constraints from the Faku ophiolite in north Liaoning, NE China: Gondwana Research, v. 103, p. 64–83.

Shi, Y., Liu, Z.H., Liu, Y.J., Shi, S.S., Wei, M.H., Yang, J.J., & Gao,T., 2019, Late Paleozoic–early Mesozoic southward subduction-closure of the Paleo-Asian Ocean: Proof from geochemistry and geochronology of early Permian–late Triassic felsic intrusive rocks from North Liaoning, NE China: Lithos, v. 346–347, p. 105165.

LBGMR (Liaoning Bureau of Geology and Mineral Resources), 1996, 1:50,000 Scale Geological Maps of Kaiyuan, Shantoupu, and Mengjiazhai (Liaoning and the related notes in Chinese with English abstract).

LBGMR (Liaoning Bureau of Geology and Mineral Resources), 2003, 1:50,000 Scale Geological Maps of Xiaertai and Changtu (Liaoning and the related notes in Chinese with English abstract).

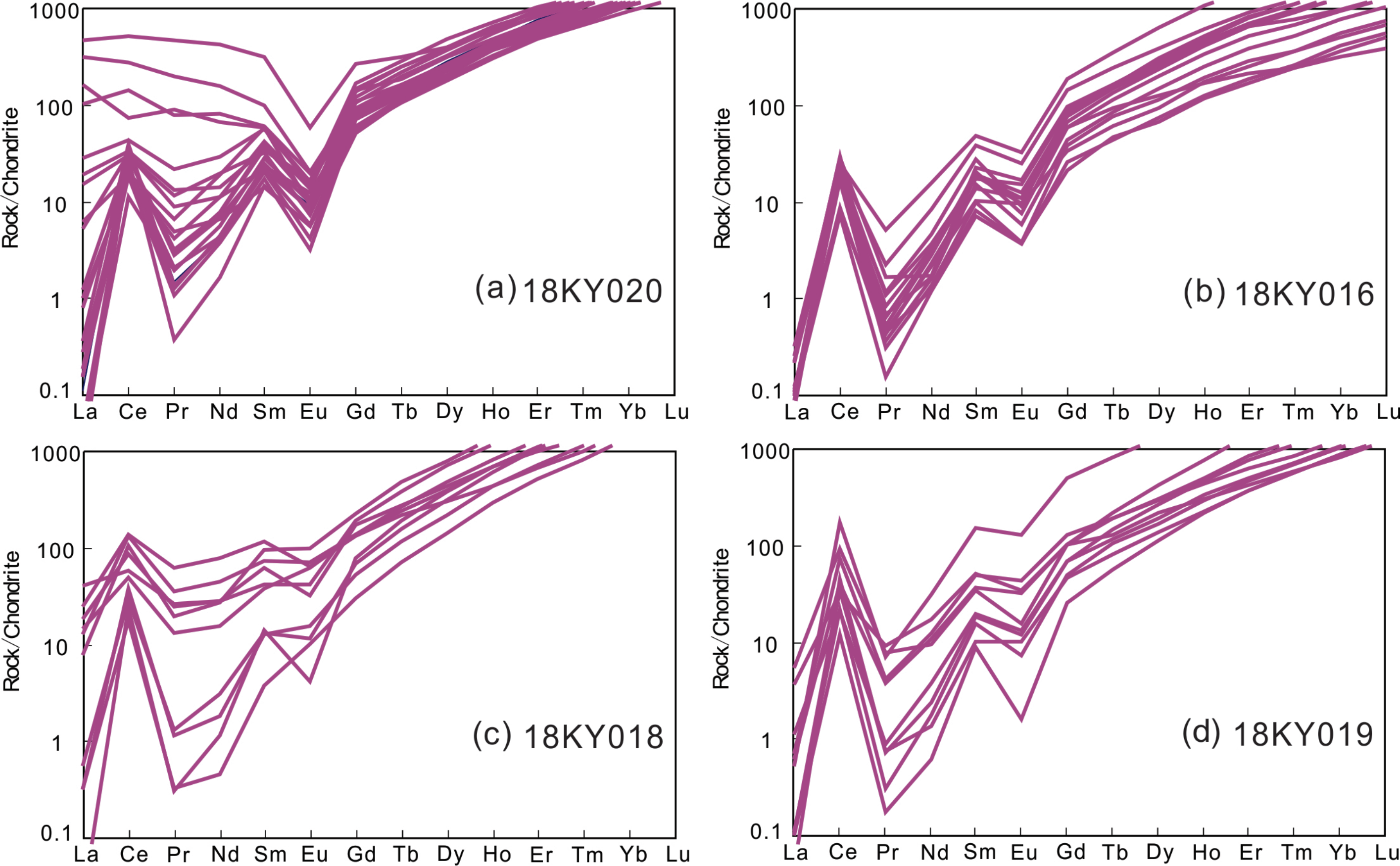

(a) 18KY020
(b) 18KY016
(c) 18KY018
(d) 18KY019
Rock/Chondrite
0.1
1
10
100
1000
La Ce Pr Nd Sm Eu Gd Tb Dy Ho Er Tm Yb Lu

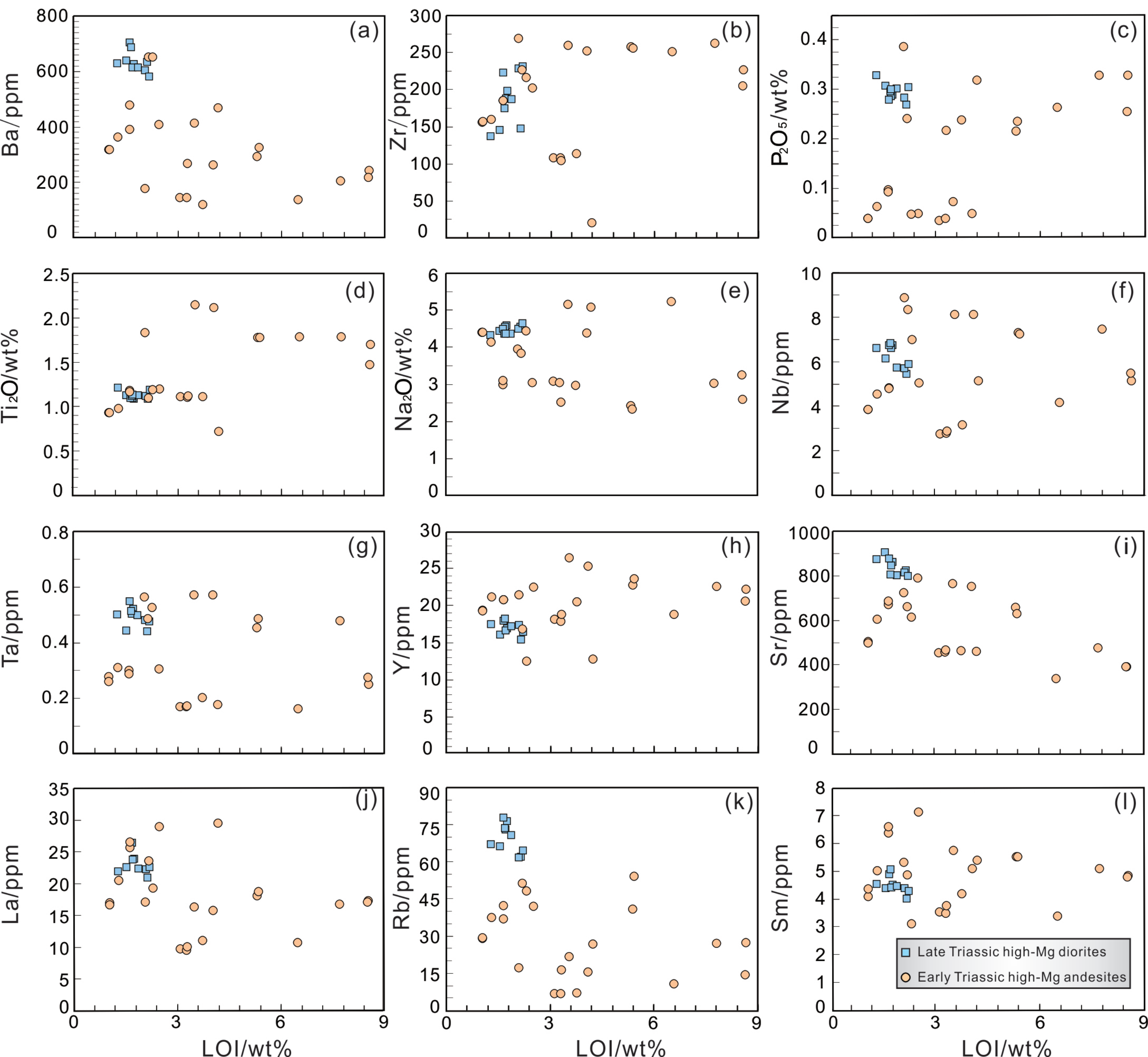

(a) Ba/ppm
(b) Zr/ppm
(c) P2O5/wt%
(d) Ti2O/wt%
(e) Na2O/wt%
(f) Nb/ppm
(g) Ta/ppm
(h) Y/ppm
(i) Sr/ppm
(j) La/ppm
(k) Rb/ppm
(l) Sm/ppm
LOI/wt%
Late Triassic high-Mg diorites
Early Triassic high-Mg andesites

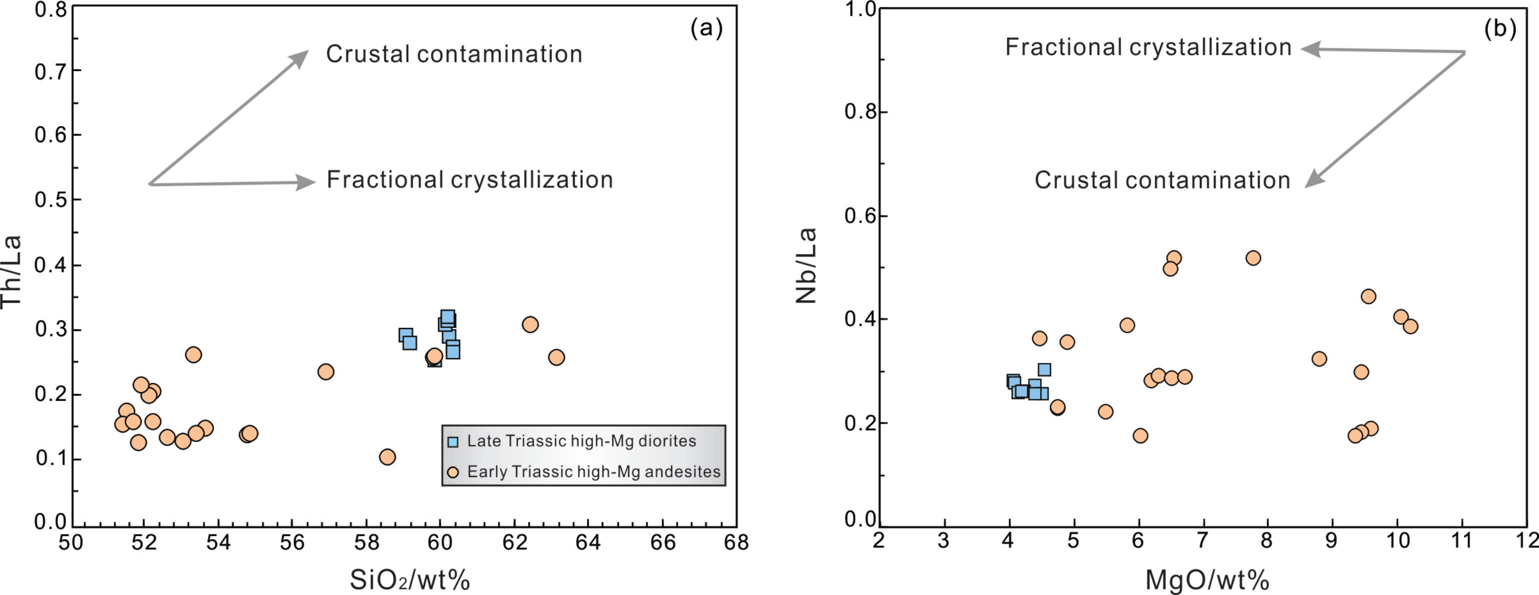

(a)
Crustal contamination
Fractional crystallization
Th/La
SiO2/wt%
Late Triassic high-Mg diorites
Early Triassic high-Mg andesites
(b)
Fractional crystallization
Crustal contamination
Nb/La
MgO/wt%

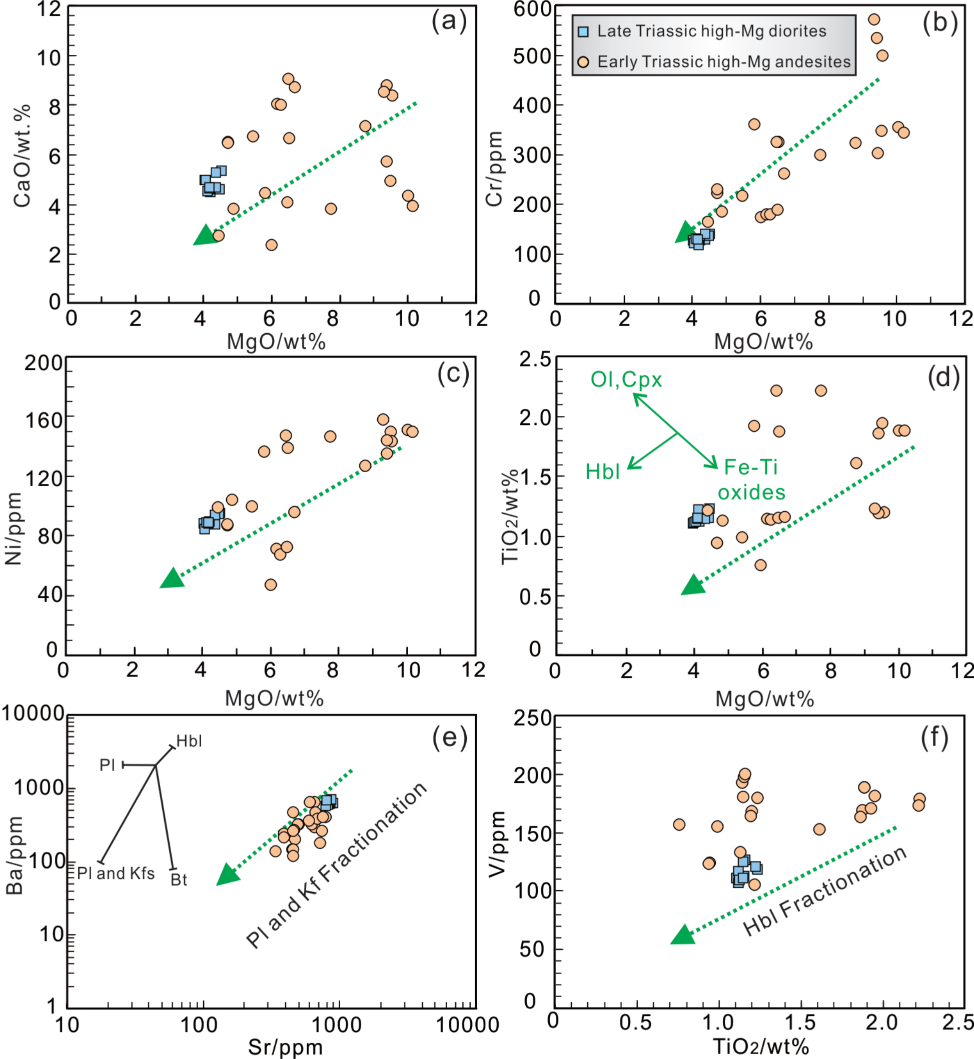

(a)
CaO/wt.%
MgO/wt%
(b)
Late Triassic high-Mg diorites
Early Triassic high-Mg andesites
Cr/ppm
MgO/wt%
(c)
Ni/ppm
MgO/wt%
(d)
Ol,Cpx
Hbl
Fe-Ti oxides
TiO2/wt%
MgO/wt%
(e)
Hbl
Pl
Pl and Kfs
Bt
Pl and Kf Fractionation
Ba/ppm
Sr/ppm
(f)
Hbl Fractionation
V/ppm
TiO2/wt%

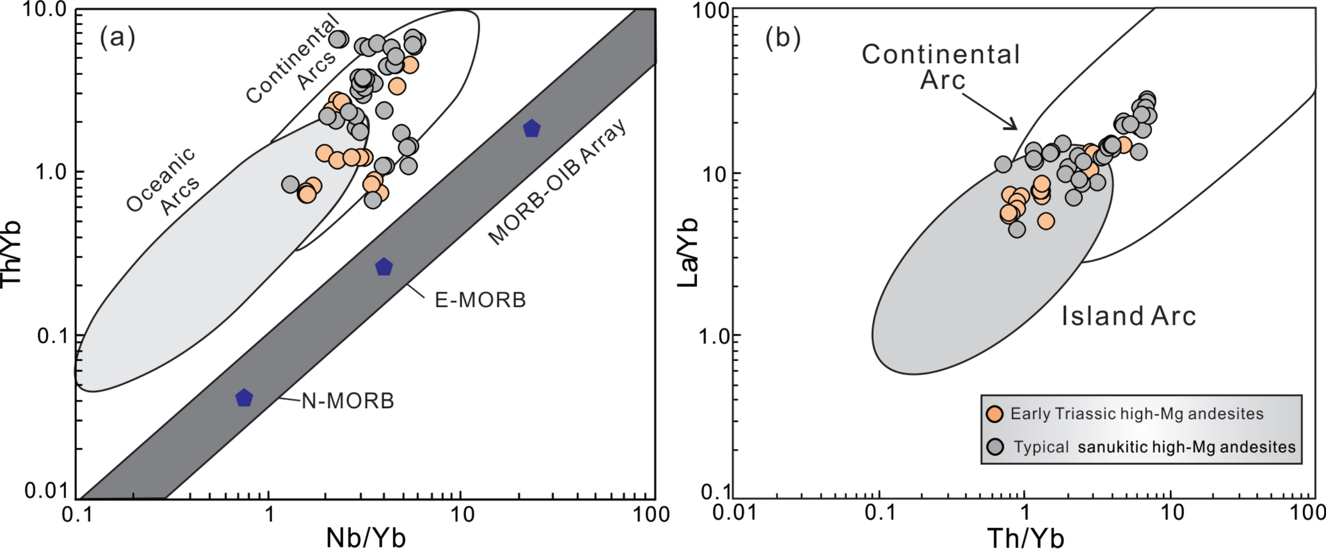

(a)
Continental Arcs
Oceanic Arcs
MORB-OIB Array
E-MORB
N-MORB
Th/Yb
Nb/Yb
10.0
1.0
0.1
0.01
0.1
1
10
100
(b)
Continental Arc
Island Arc
La/Yb
Th/Yb
100
10
1.0
0.1
0.01
0.1
1
10
100
Early Triassic high-Mg andesites
Typical sanukitic high-Mg andesites

Table S1. LA-ICP-MS and SIMS zircon U-Pb data of the Triassic high-magnesium igneous associations in the southeastern segment of the CAOB

Spot	Pb*	Th	U	Th/U	Isotopic ratios						Isotopic Ages					
					$^{207}Pb/^{206}Pb$		$^{207}Pb/^{235}U$		$^{206}Pb/^{238}U$		$^{207}Pb/^{206}Pb$		$^{207}Pb/^{235}U$		$^{206}Pb/^{238}U$	
	ppm	ppm	ppm		Ratio	1δ	Ratio	1δ	Ratio	1δ	Ages	1δ	Ages	1δ	Ages	1δ
18KY020*-1	12	177	247	0.72	0.05157	0.00209	0.27981	0.01113	0.03935	0.00063	266	62	251	9	249	4
18KY020*-2	9	160	183	0.87	0.05341	0.00288	0.28814	0.01512	0.03913	0.00074	346	84	257	12	247	5
18KY020*-3	6	69	116	0.59	0.05027	0.00290	0.27086	0.01521	0.03908	0.00076	207	94	243	12	247	5
18KY020*-4	7	95	140	0.68	0.05161	0.00287	0.27836	0.01506	0.03912	0.00075	268	89	249	12	247	5
18KY020*-5	6	60	119	0.51	0.05287	0.00504	0.28663	0.02647	0.03933	0.00111	323	157	256	21	249	7
18KY020*-6	7	118	103	1.15	0.06397	0.00292	0.39819	0.01761	0.04514	0.00081	741	63	340	13	285	5
18KY020*-7	12	209	223	0.94	0.05078	0.00263	0.27484	0.01387	0.03926	0.00071	231	83	247	11	248	4
18KY020*-8	14	193	278	0.69	0.04781	0.00168	0.25865	0.00898	0.03924	0.00058	90	54	234	7	248	4
18KY020*-9	8	94	171	0.55	0.05094	0.00671	0.27932	0.03559	0.03977	0.00149	238	217	250	28	251	9
18KY020*-10	8	97	157	0.62	0.04996	0.00269	0.26938	0.01415	0.03911	0.00072	193	87	242	11	247	4
18KY020*-11	6	81	116	0.70	0.05497	0.00309	0.29633	0.01616	0.03910	0.00076	411	87	264	13	247	5
18KY020*-12	9	118	157	0.75	0.06214	0.00442	0.32852	0.02252	0.03835	0.00074	679	157	288	17	243	5
18KY020*-13	10	128	199	0.64	0.05361	0.00341	0.28963	0.01786	0.03919	0.00083	355	101	258	14	248	5
18KY020*-14	9	135	184	0.73	0.04911	0.00441	0.26600	0.02316	0.03929	0.00104	153	146	239	19	248	6
18KY020*-15	11	126	238	0.53	0.05261	0.00280	0.28707	0.01488	0.03958	0.00074	312	84	256	12	250	5
18KY020*-16	7	87	147	0.59	0.05118	0.00293	0.27901	0.01557	0.03955	0.00076	249	93	250	12	250	5
18KY020*-17	8	116	165	0.70	0.04861	0.00304	0.26457	0.01614	0.03948	0.00079	129	100	238	13	250	5
18KY020*-18	8	100	150	0.66	0.07911	0.00589	0.43369	0.03080	0.03977	0.00108	1175	98	366	22	251	7
18KY020*-19	6	112	112	0.99	0.05364	0.00571	0.28997	0.02985	0.03922	0.00124	356	175	259	23	248	8
18KY020*-20	10	102	206	0.49	0.05010	0.00250	0.27313	0.01332	0.03955	0.00069	200	81	245	11	250	4
18KY019-1	42	212	993	0.21	0.05277	0.00195	0.28898	0.01050	0.03952	0.00059	319	55	258	8	250	4
18KY019-2	20	524	336	1.56	0.05469	0.00356	0.29879	0.01887	0.03945	0.00083	400	104	265	15	249	5

18KY019-3	59	106	97	1.09	0.15765	0.00408	9.39197	0.23973	0.43036	0.00736	2431	22	2377	23	2307	33
18KY019-4	8	138	154	0.90	0.05199	0.00283	0.28111	0.01492	0.03908	0.00072	285	88	252	12	247	4
18KY019-5	11	149	234	0.64	0.04855	0.00339	0.26328	0.01787	0.03922	0.00085	126	112	237	14	248	5
18KY019-6	11	166	211	0.79	0.07199	0.00771	0.38009	0.03929	0.03829	0.00107	986	227	327	29	242	7
18KY019-7	11	76	263	0.29	0.04812	0.00277	0.26109	0.01475	0.03933	0.00070	105	93	236	12	249	4
18KY019-8	37	570	749	0.76	0.05381	0.00245	0.29073	0.01256	0.03919	0.00056	363	105	259	10	248	4
18KY019-9	14	500	233	2.15	0.05148	0.00196	0.27823	0.01043	0.03926	0.00062	262	57	249	8	248	4
18KY019-10	26	335	595	0.56	0.05135	0.00140	0.27749	0.00757	0.03930	0.00055	257	37	249	6	248	3
18KY018-1	42	757	792	0.96	0.05991	0.00226	0.32580	0.01202	0.03939	0.00062	600	53	286	9	249	4
18KY018-2	37	238	807	0.30	0.05712	0.00151	0.31131	0.00824	0.03948	0.00054	496	35	275	6	250	3
18KY018-3	21	403	376	1.07	0.05688	0.00270	0.31159	0.01440	0.03969	0.00070	487	71	275	11	251	4
18KY018-4	15	244	299	0.82	0.05088	0.00492	0.27365	0.02566	0.03897	0.00109	235	160	246	20	246	7
18KY018-5	8	101	171	0.59	0.06008	0.00368	0.32640	0.01932	0.03937	0.00083	606	91	287	15	249	5
18KY018-6	8	137	143	0.95	0.05735	0.00594	0.31263	0.03128	0.03952	0.00124	505	166	276	24	250	8
18KY018-7	37	599	660	0.91	0.07734	0.00510	0.41039	0.02585	0.03848	0.00076	1130	135	349	19	243	5
18KY018-8	34	526	691	0.76	0.05658	0.00132	0.30897	0.00727	0.03960	0.00053	475	29	273	6	250	3
18KY018-9	13	94	294	0.32	0.05334	0.00233	0.28960	0.01237	0.03938	0.00066	343	66	258	10	249	4
18KY018-10	21	122	476	0.26	0.05320	0.00157	0.28775	0.00846	0.03925	0.00056	337	41	257	7	248	3
18KY016-1	25	22	22	0.99	0.16760	0.00560	10.76768	0.35137	0.46599	0.00986	2534	28	2503	30	2466	43
18KY016-2	36	23	36	0.65	0.15692	0.00557	9.85477	0.30417	0.45547	0.00795	2423	62	2421	28	2420	35
18KY016-3	11	5	12	0.42	0.15708	0.00690	9.86921	0.38452	0.45568	0.00922	2424	76	2423	36	2420	41
18KY016-4	5	65	72	0.90	0.05822	0.01297	0.31129	0.06682	0.03878	0.00247	538	361	275	52	245	15
18KY016-5	61	129	49	2.61	0.16295	0.00531	10.32480	0.28644	0.45953	0.00786	2487	56	2464	26	2437	35
18KY016-6	44	35	50	0.68	0.16293	0.00511	10.36988	0.27722	0.46162	0.00758	2486	54	2468	25	2447	33
18KY016-7	30	22	35	0.62	0.16133	0.00406	10.55441	0.26500	0.47452	0.00824	2470	21	2485	23	2503	36
18KY016-8	9	85	138	0.62	0.04866	0.00497	0.26808	0.02657	0.03996	0.00117	131	167	241	21	253	7

18KY016-9	15	269	213	1.26	0.05741	0.00501	0.31654	0.02679	0.03999	0.00106	507	140	279	21	253	7
18KY016-10	8	117	130	0.91	0.06599	0.01229	0.35941	0.06416	0.03950	0.00225	806	286	312	48	250	14
18KY016-11	5	72	93	0.77	0.05355	0.00789	0.28766	0.04090	0.03896	0.00167	352	241	257	32	246	10
18KY016-12	8	5	11	0.40	0.17274	0.00510	11.00508	0.31902	0.46212	0.00905	2584	24	2524	27	2449	40
18KY016-13	8	137	138	0.99	0.05203	0.00678	0.27885	0.03511	0.03887	0.00145	287	215	250	28	246	9
18KY016-14	28	38	38	0.99	0.16445	0.00384	10.66657	0.24946	0.47049	0.00787	2502	19	2495	22	2486	35
18KY016-15	9	97	179	0.54	0.05599	0.00446	0.29881	0.02301	0.03871	0.00097	452	127	265	18	245	6
18KY001-01	7	182	156	1.17	0.05308	0.00196	0.25386	0.00970	0.25390	0.00970	332	84	230	9	220	2
18KY001-02	4	129	109	1.19	0.05119	0.00436	0.23736	0.01989	0.23740	0.01990	249	196	216	18	213	2
18KY001-03	5	132	115	1.15	0.05251	0.00263	0.24729	0.01268	0.24730	0.01270	308	114	224	12	217	2
18KY001-04	8	200	179	1.11	0.04976	0.00168	0.24573	0.00836	0.24570	0.00840	184	78	223	8	227	2
18KY001-05	7	185	166	1.11	0.05145	0.00217	0.24988	0.01120	0.24990	0.01120	261	97	226	10	223	3
18KY001-06	23	687	526	1.31	0.05096	0.00085	0.24096	0.00438	0.24100	0.00440	239	39	219	4	217	2
18KY001-07	7	198	161	1.23	0.05151	0.00213	0.25113	0.01068	0.25110	0.01070	264	95	227	10	224	2
18KY001-08	8	235	189	1.24	0.04997	0.00208	0.23916	0.01015	0.23920	0.01020	193	97	218	9	220	2
18KY001-09	9	190	218	0.87	0.05174	0.00192	0.24302	0.00902	0.24300	0.00900	274	85	221	8	216	2
18KY001-10	6	146	127	1.15	0.05184	0.00272	0.25001	0.01345	0.25000	0.01340	278	120	227	12	222	3
18KY001-11	5	126	107	1.18	0.05005	0.00316	0.24609	0.01569	0.24610	0.01570	197	147	223	14	226	3
18KY001-12	11	239	262	0.91	0.05144	0.00139	0.25109	0.00701	0.25110	0.00700	261	62	227	6	224	3
18KY001-13	8	217	175	1.24	0.05251	0.00187	0.25311	0.00916	0.25310	0.00920	308	81	229	8	221	2
18KY001-14	9	206	214	0.96	0.05114	0.00187	0.25109	0.00987	0.25110	0.00990	247	84	227	9	226	3
18KY001-15	11	329	257	1.28	0.05233	0.00140	0.25069	0.00691	0.25070	0.00690	300	61	227	6	220	2
18KY001-16	8	219	193	1.14	0.05054	0.00170	0.24047	0.00820	0.24050	0.00820	220	78	219	7	219	2
18KY001-17	11	286	251	1.14	0.04922	0.00213	0.24503	0.01064	0.24500	0.01060	158	101	223	10	229	3
18KY001-18	16	466	351	1.33	0.05014	0.00135	0.24712	0.00680	0.24710	0.00680	201	62	224	6	226	3
18KY001-19	16	407	350	1.16	0.04928	0.00125	0.24452	0.00668	0.24450	0.00670	161	59	222	6	228	3

18KY001-20	8	207	177	1.17	0.05170	0.00243	0.24889	0.01212	0.24890	0.01210	272	108	226	11	221	3
18KY001-21	5	100	129	0.78	0.05038	0.00266	0.24489	0.01292	0.24490	0.01290	212	122	222	12	223	2
18KY001-22	6	170	155	1.10	0.05248	0.00217	0.24345	0.01025	0.24340	0.01020	306	94	221	9	213	2
18KY001-23	30	725	709	1.02	0.05137	0.00082	0.25042	0.00437	0.25040	0.00440	258	36	227	4	224	3
18KY001-24	14	322	338	0.95	0.05012	0.00128	0.23435	0.00635	0.23440	0.00630	200	59	214	6	215	2
18KY006-01	9	216	223	0.97	0.04880	0.00147	0.23748	0.00737	0.03530	0.00039	138	71	216	7	224	2
18KY006-02	20	528	469	1.12	0.05078	0.00092	0.24711	0.00469	0.03529	0.00039	231	42	224	4	224	2
18KY006-03	11	297	255	1.17	0.04884	0.00125	0.23574	0.00623	0.03500	0.00038	140	60	215	6	222	2
18KY006-04	13	200	348	0.58	0.04965	0.00117	0.23719	0.00603	0.03465	0.00038	178	55	216	5	220	2
18KY006-05	16	373	376	0.99	0.05124	0.00101	0.24786	0.00517	0.03508	0.00038	252	45	225	5	222	2
18KY006-06	12	241	291	0.83	0.05118	0.00244	0.24940	0.01179	0.03534	0.00040	249	110	226	11	224	3
18KY006-07	19	441	433	1.02	0.05042	0.00110	0.24960	0.00549	0.03590	0.00039	214	51	226	5	227	2
18KY006-08	3	44	79	0.56	0.04982	0.00456	0.24650	0.02246	0.03588	0.00045	187	213	224	20	227	3
18KY006-10	11	239	267	0.90	0.05062	0.00128	0.24635	0.00654	0.03529	0.00039	224	58	224	6	224	3
18KY006-11	38	982	895	1.10	0.04919	0.00071	0.23562	0.00370	0.03474	0.00039	157	34	215	3	220	2
18KY006-12	11	213	266	0.80	0.04955	0.00122	0.24603	0.00626	0.03601	0.00040	174	57	223	6	228	3
18KY006-13	10	223	244	0.92	0.04914	0.00147	0.24225	0.00745	0.03575	0.00039	155	70	220	7	226	2
18KY006-14	8	166	198	0.84	0.05118	0.00190	0.25097	0.00968	0.03556	0.00040	249	85	227	9	225	3
18KY006-15	16	442	366	1.21	0.05140	0.00111	0.25087	0.00565	0.03540	0.00038	259	50	227	5	224	2
18KY006-16	7	146	174	0.84	0.05041	0.00185	0.24903	0.00947	0.03583	0.00041	214	85	226	9	227	3
18KY006-17	4	81	109	0.74	0.05051	0.00274	0.24911	0.01360	0.03577	0.00041	219	126	226	12	227	3
18KY006-18	6	150	158	0.95	0.04993	0.00194	0.23471	0.00920	0.03409	0.00039	192	90	214	8	216	2
18KY006-19	6	98	158	0.62	0.05166	0.00210	0.24102	0.00998	0.03384	0.00037	270	93	219	9	215	2
18KY006-20	8	113	218	0.52	0.05108	0.00142	0.23843	0.00688	0.03385	0.00039	244	64	217	6	215	2
18KY006-21	17	492	412	1.19	0.04928	0.00111	0.23488	0.00539	0.03457	0.00036	161	53	214	5	219	2
18KY006-22	9	248	206	1.20	0.05192	0.00153	0.25406	0.00768	0.03549	0.00039	282	67	230	7	225	2

18KY006-23	16	508	357	1.42	0.05129	0.00113	0.24648	0.00564	0.03485	0.00039	254	51	224	5	221	2
18KY006-24	32	867	736	1.18	0.05069	0.00083	0.24753	0.00441	0.03542	0.00040	227	38	225	4	224	3

Spot	Pb* ppm	Th ppm	U ppm	Th/U	Isotopic ratios $^{207}Pb/^{206}Pb$ Ratio	δ %	$^{207}Pb/^{235}U$ Ratio	δ %	$^{206}Pb/^{238}U$ Ratio	δ %	Isotopic Ages $^{207}Pb/^{235}U$ Ages	1δ	$^{206}Pb/^{238}U$ Ages	1δ
18KY020@01	31	507	606	0.84	0.05070	1.47	0.27252	2.16	0.0390	1.58	244.7	4.7	246.5	3.8
18KY020@02	18	306	334	0.92	0.05264	1.94	0.28413	2.48	0.0391	1.54	253.9	5.6	247.5	3.8
18KY020@03	12	165	247	0.67	0.05012	3.21	0.27164	3.57	0.0393	1.58	244.0	7.8	248.6	3.8
18KY020@04	12	148	237	0.62	0.05103	3.18	0.27346	3.56	0.0389	1.61	245.5	7.8	245.8	3.9
18KY020@05	28	261	588	0.44	0.05081	1.52	0.27380	2.16	0.0391	1.53	245.7	4.7	247.1	3.7
18KY020@06	24	354	387	0.92	0.05347	1.96	0.33245	2.50	0.0451	1.54	291.4	6.3	284.3	4.3
18KY020@07	17	239	339	0.71	0.05096	2.60	0.27291	3.04	0.0388	1.56	245.0	6.6	245.6	3.8
18KY020@08	24	415	460	0.90	0.04770	4.61	0.25998	4.87	0.0395	1.55	234.7	10.2	249.9	3.8
18KY020@09	9	110	181	0.61	0.05207	2.81	0.28225	3.23	0.0393	1.59	252.4	7.2	248.6	3.9
18KY020@10	18	261	346	0.75	0.05069	2.64	0.27544	3.07	0.0394	1.56	247.0	6.8	249.2	3.8
18KY020@11	14	225	264	0.85	0.05056	2.48	0.27006	2.91	0.0387	1.53	242.7	6.3	245.0	3.7
18KY020@12	26	400	489	0.82	0.05047	1.72	0.27750	2.30	0.0399	1.52	248.7	5.1	252.1	3.8
18KY020@13	18	207	376	0.55	0.04978	2.10	0.26874	2.61	0.0392	1.55	241.7	5.6	247.6	3.8
18KY020@14	23	338	459	0.74	0.05347	1.95	0.28613	2.51	0.0388	1.57	255.5	5.7	245.5	3.8
18KY020@15	10	111	214	0.52	0.05089	2.57	0.27395	3.08	0.0390	1.69	245.8	6.7	246.9	4.1
18KY020@16	14	166	298	0.56	0.05058	2.21	0.26987	2.71	0.0387	1.56	242.6	5.9	244.7	3.7
18KY020@17	9	101	191	0.53	0.05361	3.09	0.28579	3.48	0.0387	1.60	255.2	7.9	244.5	3.8
18KY020@18	14	180	277	0.65	0.05248	2.23	0.28287	2.72	0.0391	1.55	252.9	6.1	247.2	3.8
18KY020@19	16	303	306	0.99	0.05076	2.68	0.27088	3.10	0.0387	1.55	243.4	6.7	244.8	3.7
18KY020@20	16	157	338	0.46	0.05056	2.10	0.26888	2.62	0.0386	1.57	241.8	5.7	243.9	3.8

Table S2. Major (wt%) and trace (ppm) elements of the Triassic high-magnesium igneous associations in the southeastern segment of the CAOB

Sample	18KY001	18KY001-1	18KY002	18KY002-1	18KY003	18KY003-1	18KY003-1*	18KY004	18KY004-1	18KY006	18KY007	18KY007*	17KY01	17KY03	16KY001	16KY002	16KY003
Rocks	Diorite						Quartz diorite						Andesite				
SiO_2	58.24	58.07	59.41	59.08	58.96	58.53		58.98	58.42	59.18	59.05	59.28	57.30	61.54	47.41	49.69	46.95
TiO_2	1.21	1.13	1.09	1.10	1.13	1.09		1.12	1.19	1.10	1.12	1.14	1.83	1.10	1.79	1.79	1.70
Al_2O_3	16.57	16.73	16.70	16.63	16.25	16.78		16.51	16.84	16.36	16.16	16.19	12.70	13.99	15.32	15.68	15.12
Fe_2O_3T	5.90	5.70	5.22	5.19	5.66	5.29		5.55	5.42	5.42	5.51	5.58	7.76	5.72	9.61	10.18	9.47
MnO	0.09	0.08	0.08	0.08	0.08	0.08		0.08	0.08	0.08	0.08	0.08	0.11	0.07	0.11	0.10	0.12
MgO	4.48	4.31	4.00	4.00	4.42	4.11		4.31	4.10	4.05	4.10	4.12	6.40	4.77	8.78	5.43	8.62
CaO	5.29	5.20	4.93	4.90	4.54	4.38		4.61	4.51	4.45	4.57	4.62	6.53	3.73	4.56	4.18	5.23
Na_2O	4.33	4.44	4.58	4.55	4.36	4.55		4.49	4.65	4.49	4.36	4.36	3.95	3.84	3.02	5.23	2.60
K_2O	2.15	2.15	2.30	2.29	2.33	2.15		2.01	2.12	2.67	2.62	2.66	0.83	2.44	1.06	0.60	1.19
P_2O_5	0.33	0.31	0.29	0.29	0.30	0.27		0.28	0.30	0.28	0.30	0.30	0.39	0.24	0.33	0.26	0.33
LOI	1.28	1.53	1.75	1.71	1.87	2.14		2.09	2.20	1.64	1.68	1.71	2.07	2.17	7.74	6.52	8.57
SUM	99.87	99.64	100.34	99.80	99.89	99.36		100.04	99.84	99.70	99.55	100.03	99.87	99.61	99.73	99.67	99.90
Li	24.0	22.8	19.3	19.0	21.8	22.3	22.6	22.1	22.9	22.0	20.3		31.5	22.4	40.2	27.0	35.6
Sc	13.9	12.7	12.0	11.9	13.0	11.5	11.7	13.1	11.9	12.0	12.0		19.6	14.0	25.5	23.1	22.9
V	118	112	110	106	126	116	116	124	120	109	110		169	133	181	170	163
Cr	139	129	127	122	137	127	131	140	117	132	130		325	184	347	361	302
Co	22.0	21.0	19.5	19.1	21.0	19.6	19.9	20.8	20.0	19.8	18.6		36.2	24.4	46.3	40.2	43.3
Ni	98	90	90	87	97	92	91	97	91	91	91		143	107	154	140	139
Cu	46.4	48.3	23.3	21.8	27.6	34.9	36.3	25.6	32.8	43.3	43.3		33.8	21.9	58.7	32.3	52.5
Zn	61.1	58.7	52.5	51.4	57.9	53.6	56.3	57.7	56.0	57.4	57.0		74.2	62.9	104.0	90.0	96.4
Ga	19.9	19.6	19.8	19.4	19.4	19.8	20.0	20.0	20.0	19.9	20.1		17.0	19.0	17.6	16.4	15.7
Rb	67.3	66.3	76.6	73.1	70.8	62.2	63.9	61.8	64.6	78.0	73.6		17.17	51.40	27.20	10.70	27.40

Sr	874	905	862	847	802	824	838	816	800	878	805	725	660	477	340	391
Y	17.5	16.0	17.0	16.7	17.2	15.4	15.7	17.4	16.4	18.0	18.2	21.5	16.9	22.6	18.8	22.2
Zr	137	146	199	188	187	147	154	228	231	223	175	269	226	262	251	227
Nb	6.62	6.13	6.74	6.60	5.72	5.46	5.56	5.72	5.89	6.75	6.84	8.86	8.34	7.45	4.17	5.13
Sn	1.49	1.47	1.50	1.51	1.48	1.29	1.31	1.50	1.35	1.54	1.50			0.07	0.06	0.06
Cs	4.02	3.96	5.46	5.38	5.02	3.78	3.94	4.24	3.45	3.13	2.73	1.68	1.90	5.43	0.88	3.45
Ba	630	640	628	613	615	636	641	604	583	705	687	178	652	205	139	243
La	22.0	22.6	23.9	23.8	22.4	21.0	21.2	22.3	22.6	26.3	26.4	17.1	23.6	16.8	10.8	17.3
Ce	48.6	47.9	50.4	48.8	47.8	45.1	44.7	48.5	48.7	53.7	53.2	42.0	48.6	38.9	26.1	38.2
Pr	5.70	5.65	5.78	5.54	5.60	5.10	5.11	5.58	5.58	6.08	6.12	5.78	6.14	5.34	3.48	5.06
Nd	23.9	22.8	23.1	22.5	22.4	20.5	20.7	22.1	22.1	23.9	24.5	23.9	23.8	23.9	15.4	22.3
Sm	4.53	4.40	4.51	4.41	4.47	4.00	4.25	4.38	4.29	4.88	5.07	5.31	4.87	5.09	3.39	4.84
Eu	1.59	1.53	1.59	1.58	1.57	1.56	1.65	1.61	1.66	1.63	1.52	1.75	1.45	1.59	1.11	1.53
Gd	4.38	4.05	4.14	4.06	4.05	3.67	3.76	4.23	3.93	4.33	4.35	5.42	4.69	4.54	3.21	4.46
Tb	0.61	0.58	0.59	0.56	0.59	0.54	0.53	0.59	0.55	0.62	0.64	0.81	0.66	0.82	0.62	0.78
Dy	3.36	3.13	3.22	3.26	3.17	2.98	2.96	3.19	3.06	3.60	3.50	4.90	3.91	4.39	3.37	4.16
Ho	0.64	0.58	0.64	0.61	0.63	0.56	0.56	0.66	0.61	0.68	0.67	0.98	0.77	0.86	0.69	0.81
Er	1.73	1.59	1.74	1.64	1.69	1.55	1.53	1.74	1.64	1.85	1.79	2.66	2.08	2.34	1.95	2.23
Tm	0.23	0.21	0.22	0.22	0.22	0.21	0.20	0.24	0.21	0.25	0.23	0.38	0.30	0.39	0.35	0.37
Yb	1.47	1.38	1.50	1.44	1.49	1.33	1.35	1.51	1.45	1.54	1.53	2.36	1.82	2.38	2.14	2.25
Lu	0.21	0.20	0.22	0.21	0.22	0.20	0.19	0.22	0.21	0.23	0.23	0.36	0.28	0.36	0.32	0.32
Hf	3.27	3.41	4.56	4.41	4.32	3.46	3.48	5.28	4.93	4.98	3.99	6.52	5.23	5.02	4.98	4.66
Ta	0.50	0.44	0.52	0.50	0.50	0.44	0.46	0.48	0.48	0.55	0.51	0.56	0.49	0.48	0.16	0.25
Tl	0.45	0.46	0.57	0.53	0.51	0.44	0.42	0.39	0.42	0.56	0.52			0.25	0.12	0.23
Pb	11.9	12.3	12.4	11.9	12.9	13.4	14.1	13.5	13.3	14.4	13.9	5.5	10.0	9.0	6.6	7.9

Th	6.44	6.36	7.56	6.93	6.92	6.64	6.99	7.18	5.74	7.22	7.04		1.77	6.09	2.95	2.84	2.66
U	1.99	1.95	2.08	2.13	2.21	2.55	2.34	2.26	2.01	2.54	2.42		0.52	2.14	0.81	0.86	0.68

*means duplicate sample

Table S2. Major (wt.%) and trace (ppm) elements of the Triassic high-magnesium igneous associations in the southeastern CAOB

Sample	16KY004	16KY005	16KY006	16KY007	16KY008	16KY009	16KY010	18FK067	18KY016	18KY017	18KY019	18KY020	18KY020-1	18FK067-1	18FK067-2	18FK068	18FK068*
Rocks	Andesite																
SiO_2	49.39	48.87	48.96	51.36	51.24	56.16	50.58	53.13	50.07	50.65	60.97	59.17	59.38	53.26	51.60	50.92	
TiO_2	1.78	1.78	1.47	1.18	1.17	0.98	1.20	1.11	2.15	2.12	1.19	0.93	0.93	1.10	1.11	1.12	
Al_2O_3	15.83	15.97	13.85	14.62	14.60	16.26	14.72	16.18	17.35	16.70	16.14	15.85	15.86	16.37	15.83	16.54	
Fe_2O_3T	9.85	10.13	8.16	8.68	8.61	7.34	8.77	9.05	10.40	9.69	5.65	6.03	6.06	8.82	9.29	9.44	
MnO	0.12	0.12	0.13	0.14	0.14	0.12	0.13	0.13	0.08	0.09	0.06	0.10	0.10	0.13	0.13	0.14	
MgO	9.50	9.64	8.03	9.43	9.27	5.41	9.10	6.01	6.26	7.42	4.37	4.70	4.70	6.12	6.29	6.50	
CaO	4.14	3.73	6.52	8.25	8.63	6.65	8.31	7.79	3.95	3.68	2.68	6.44	6.45	7.77	8.75	8.43	
Na_2O	2.43	2.34	3.25	3.00	3.11	4.14	3.04	3.08	5.16	4.38	4.43	4.40	4.40	3.04	2.97	2.53	
K_2O	1.33	1.72	0.63	1.58	1.42	1.55	1.52	0.46	1.09	0.71	2.12	1.30	1.28	0.44	0.41	0.93	
P_2O_5	0.22	0.24	0.26	0.10	0.09	0.06	0.05	0.04	0.07	0.05	0.05	0.04	0.04	0.04	0.24	0.22	
LOI	5.33	5.38	8.55	1.63	1.63	1.30	2.49	3.09	3.51	4.06	2.30	1.03	1.04	3.29	3.74	3.31	
SUM	99.91	99.91	99.81	99.97	99.91	99.97	99.91	100.07	100.08	99.55	99.96	99.98	100.24	100.38	100.37	100.08	
Li	38.8	38.9	31.7	23.2	16.6	12.5	25.8	24.0	24.0	27.6	18.4	9.8	9.9	23.9	22.7	23.8	23.2
Sc	24.1	24.1	21.2	23.3	23.4	19.9	26.5	26.0	26.0	25.5	15.5	19.4	19.0	25.4	23.6	25.1	25.6
V	188	188	152	168	164	155	179	180	178	173	105	123	123	193	198	200	200
Cr	355	343	324	499	534	216	572	180	326	298	165	222	230	179	189	262	264
Co	47.8	48.4	37.6	41.4	40.0	28.6	44.9	31.9	37.3	37.9	21.3	22.6	23.1	31.6	33.0	35.0	34.3
Ni	155	154	130	147	148	102	162	73	151	151	102	89	90	69	74	98	98

Cu	53.8	38.3	15.9	24.9	26.3	20.6	27.1	10.9	17.1	18.0	31.5	9.3	9.0	10.0	171.5	42.0	42.2
Zn	103.0	107.0	85.7	92.9	92.3	79.8	95.9	84.8	75.9	75.7	52.1	55.6	54.9	83.4	88.4	90.0	88.9
Ga	17.4	17.8	14.9	15.9	16.4	19.8	16.8	19.3	19.0	18.4	18.8	18.0	17.9	18.5	18.3	19.1	19.4
Rb	40.9	54.2	14.5	42.2	36.9	37.4	42.0	6.9	21.8	15.5	48.1	29.1	29.2	6.8	7.1	16.3	15.8
Sr	659	630	392	670	688	604	791	453	764	752	614	505	499	458	463	466	462
Y	22.8	23.6	20.6	20.8	20.8	21.2	22.5	18.1	26.4	25.3	12.5	19.4	19.3	17.9	20.5	18.8	19.0
Zr	258	256	205	185	185	160	202	108	259	252	216	156	157	108	114	104	106
Nb	7.29	7.23	5.50	4.84	4.81	4.55	5.06	2.75	8.11	8.13	7.00	3.87	3.86	2.79	3.18	2.89	2.89
Sn	0.06	0.07	0.05	0.05	0.05	0.05	0.06	0.85	2.16	2.29	1.57	1.31	1.29	1.16	1.48	1.12	1.08
Cs	24.40	33.70	6.28	3.57	2.61	2.61	3.02	0.63	3.44	2.80	1.95	0.96	0.93	0.61	0.95	1.61	1.63
Ba	294	326	217	480	390	364	410	146	413	263	652	320	320	145	120	268	267
La	18.1	18.8	17.1	25.7	26.5	20.5	29.0	9.7	16.4	15.8	19.3	17.0	16.7	9.6	11.1	10.1	10.2
Ce	42.3	43.0	38.3	56.6	57.9	42.6	64.1	22.9	40.3	39.4	35.7	37.7	37.0	22.8	27.7	24.6	24.6
Pr	5.75	5.79	5.15	7.30	7.61	5.49	8.34	3.07	5.32	5.12	3.94	4.63	4.66	3.10	3.70	3.29	3.17
Nd	25.2	25.6	22.6	32.8	33.8	24.3	36.4	14.1	22.8	22.1	15.1	20.0	19.2	14.3	17.1	15.7	14.7
Sm	5.51	5.51	4.80	6.38	6.59	5.01	7.12	3.53	5.75	5.10	3.11	4.09	4.36	3.48	4.20	3.75	3.60
Eu	1.91	1.85	1.56	1.91	1.95	1.57	2.11	1.19	1.78	1.67	1.12	1.31	1.39	1.20	1.25	1.24	1.20
Gd	4.78	4.79	4.23	5.27	5.09	4.59	6.00	3.34	4.92	4.67	2.61	3.99	3.89	3.24	3.82	3.57	3.76
Tb	0.84	0.87	0.77	0.85	0.83	0.78	0.95	0.59	0.88	0.80	0.41	0.65	0.57	0.51	0.57	0.55	0.57
Dy	4.37	4.50	4.06	4.07	4.06	3.88	4.43	3.28	5.05	4.87	2.35	3.71	3.58	3.34	3.92	3.41	3.44
Ho	0.83	0.87	0.74	0.75	0.75	0.73	0.79	0.66	0.96	0.91	0.48	0.71	0.68	0.67	0.76	0.66	0.66
Er	2.32	2.39	2.05	2.01	2.00	2.01	2.20	1.84	2.60	2.60	1.29	1.96	1.88	1.81	2.11	1.85	1.83
Tm	0.38	0.39	0.34	0.32	0.33	0.35	0.36	0.23	0.36	0.30	0.17	0.27	0.27	0.25	0.29	0.26	0.28
Yb	2.33	2.43	2.03	2.05	1.99	2.14	2.24	1.62	2.32	2.40	1.31	1.83	1.62	1.77	2.02	1.85	1.83
Lu	0.34	0.35	0.28	0.28	0.28	0.31	0.31	0.28	0.42	0.36	0.20	0.30	0.29	0.26	0.30	0.27	0.28

Hf	5.01	5.27	4.22	4.35	4.31	3.94	4.63	2.80	5.63	5.37	4.98	3.81	3.83	2.71	2.87	2.65	2.88
Ta	0.45	0.49	0.28	0.30	0.29	0.31	0.31	0.17	0.57	0.57	0.53	0.28	0.26	0.17	0.20	0.17	0.16
Tl	0.46	0.59	0.13	0.32	0.25	0.27	0.31	0.04	0.18	0.13	0.23	0.16	0.19	0.05	0.04	0.08	0.08
Pb	9.2	9.3	6.7	9.7	11.0	12.3	10.6	5.9	8.1	7.0	8.5	11.4	10.9	6.3	8.2	6.4	6.5
Th	2.89	2.99	2.53	5.31	5.29	4.83	6.24	1.35	2.08	2.02	5.99	4.40	4.34	1.34	1.55	1.36	1.35
U	0.76	0.77	0.70	1.44	1.39	1.54	1.52	0.49	0.25	0.21	1.70	1.58	1.52	0.52	0.55	0.49	0.48

*means duplicate sample

Table S3. *In situ* zircon Hf isotopic compositions of the Triassic high-magnesium igneous associations in the southeastern segment of the CAOB

Sample No.	t (Ma)	$^{176}Yb/^{177}Hf$	2σ	$^{176}Lu/^{177}Hf$	2σ	$^{176}Hf/^{177}Hf$	2σ	$\varepsilon_{Hf}(0)$	2σ	$\varepsilon_{Hf}(t)$	2σ	T_{DM1}	2σ	T_{DM2}	2σ	$f_{Lu/Hf}$
18KY001-01	220	0.033462	0.000389	0.000890	0.000004	0.282856	0.000021	2.97	0.73	7.67	0.73	560	29	762	47	-0.97
18KY001-02	213	0.025801	0.000156	0.000697	0.000006	0.282838	0.000028	2.33	1.00	6.92	1.01	582	40	805	64	-0.98
18KY001-03	217	0.030307	0.000444	0.000828	0.000006	0.282899	0.000020	4.47	0.71	9.12	0.71	499	28	668	45	-0.98
18KY001-04	227	0.046133	0.000477	0.001262	0.000005	0.282802	0.000024	1.07	0.84	5.86	0.84	642	34	883	54	-0.96
18KY001-05	223	0.056006	0.000976	0.001457	0.000011	0.282889	0.000021	4.15	0.74	8.84	0.74	520	30	690	47	-0.96
18KY001-06	217	0.073260	0.000354	0.001944	0.000022	0.282829	0.000023	2.02	0.82	6.52	0.82	615	34	834	52	-0.94
18KY001-07	224	0.043313	0.001085	0.001123	0.000016	0.282930	0.000022	5.60	0.79	10.36	0.79	457	32	594	50	-0.97
18KY001-08	220	0.030672	0.000250	0.000788	0.000005	0.282862	0.000019	3.18	0.68	7.90	0.68	550	27	748	43	-0.98
18KY001-09	216	0.039392	0.000626	0.001008	0.000007	0.282875	0.000028	3.64	0.98	8.24	0.98	535	39	723	63	-0.97
18KY001-10	222	0.026828	0.000603	0.000759	0.000014	0.282810	0.000021	1.35	0.76	6.11	0.76	622	30	863	48	-0.98
18KY001-11	226	0.037199	0.000311	0.001046	0.000002	0.282857	0.000024	3.00	0.85	7.81	0.86	561	34	758	55	-0.97
18KY001-12	224	0.032532	0.000104	0.000989	0.000005	0.282781	0.000021	0.32	0.75	5.10	0.75	667	30	929	47	-0.97
18KY001-13	221	0.042410	0.000328	0.001168	0.000001	0.282834	0.000025	2.21	0.89	6.90	0.89	595	36	813	57	-0.96
18KY001-14	226	0.035591	0.000746	0.000999	0.000013	0.282874	0.000022	3.60	0.78	8.41	0.78	536	31	720	50	-0.97
18KY001-15	220	0.040220	0.000263	0.001089	0.000002	0.282864	0.000024	3.25	0.85	7.93	0.85	551	34	746	54	-0.97
18KY001-16	219	0.027612	0.000113	0.000786	0.000004	0.282889	0.000021	4.12	0.76	8.82	0.76	512	30	688	48	-0.98
18KY001-17	229	0.047015	0.000302	0.001288	0.000022	0.282849	0.000021	2.73	0.75	7.56	0.75	575	30	776	48	-0.96
18KY001-18	226	0.056365	0.000786	0.001586	0.000011	0.282851	0.000024	2.79	0.86	7.53	0.86	578	35	776	55	-0.95
18KY001-19	228	0.044550	0.000181	0.001284	0.000012	0.282945	0.000024	6.12	0.86	10.94	0.86	438	35	560	55	-0.96
18KY001-20	221	0.037043	0.000558	0.001027	0.000008	0.282770	0.000023	-0.07	0.80	4.64	0.80	683	32	956	51	-0.97
18KY001-21	223	0.027435	0.000259	0.000830	0.000002	0.282836	0.000022	2.25	0.78	7.04	0.78	587	31	805	50	-0.97

18KY001-22	213	0.032444	0.001353	0.000852	0.000028	0.282828	0.000023	1.99	0.81	6.55	0.81	598	32	829	52	-0.97
18KY001-23	224	0.049994	0.000479	0.001335	0.000002	0.282877	0.000020	3.71	0.70	8.43	0.70	537	28	717	45	-0.96
18KY001-24	215	0.039484	0.001916	0.001032	0.000041	0.282850	0.000019	2.78	0.67	7.35	0.67	570	27	779	43	-0.97
18KY006-01	224	0.049431	0.000614	0.001221	0.000005	0.282918	0.000026	5.18	0.93	9.91	0.93	476	37	622	59	-0.96
18KY006-02	224	0.022132	0.000061	0.000656	0.000004	0.282786	0.000023	0.50	0.80	5.31	0.80	654	32	915	51	-0.98
18KY006-03	222	0.036531	0.000208	0.000972	0.000003	0.282864	0.000023	3.24	0.80	7.97	0.81	550	32	745	51	-0.97
18KY006-04	220	0.021702	0.000082	0.000624	0.000008	0.282865	0.000020	3.30	0.71	8.04	0.71	543	28	739	45	-0.98
18KY006-05	222	0.053133	0.000756	0.001416	0.000007	0.282882	0.000024	3.87	0.86	8.55	0.86	531	35	708	55	-0.96
18KY006-06	224	0.018485	0.000127	0.000507	0.000001	0.282814	0.000022	1.48	0.77	6.33	0.77	613	30	851	49	-0.98
18KY006-07	227	0.056373	0.000927	0.001474	0.000010	0.282843	0.000024	2.49	0.83	7.27	0.83	588	34	794	53	-0.96
18KY006-08	227	0.014521	0.000233	0.000396	0.000001	0.282830	0.000024	2.04	0.83	6.98	0.84	589	33	812	53	-0.99
18KY006-10	224	0.048240	0.000915	0.001139	0.000007	0.282836	0.000021	2.25	0.73	7.00	0.73	592	29	808	47	-0.97
18KY006-11	220	0.050615	0.000483	0.001295	0.000001	0.282908	0.000019	4.80	0.68	9.45	0.68	492	27	649	43	-0.96
18KY006-12	228	0.027123	0.000174	0.000744	0.000001	0.282821	0.000021	1.74	0.76	6.64	0.76	606	30	834	48	-0.98
18KY006-13	226	0.064315	0.000365	0.001735	0.000005	0.282859	0.000025	3.08	0.88	7.80	0.88	568	36	760	56	-0.95
18KY006-14	225	0.021152	0.000093	0.000583	0.000003	0.282853	0.000020	2.87	0.71	7.74	0.71	559	28	762	45	-0.98
18KY006-15	224	0.045691	0.000214	0.001263	0.000004	0.282836	0.000021	2.28	0.76	7.02	0.76	593	31	807	48	-0.96
18KY006-16	227	0.020322	0.000162	0.000558	0.000001	0.282839	0.000023	2.37	0.80	7.27	0.80	579	32	793	51	-0.98
18KY006-17	227	0.024550	0.000194	0.000660	0.000007	0.282783	0.000021	0.38	0.76	5.26	0.76	659	30	921	48	-0.98
18KY006-18	216	0.019857	0.000085	0.000555	0.000002	0.282922	0.000023	5.31	0.80	9.98	0.81	462	32	612	51	-0.98
18KY006-19	215	0.029253	0.000064	0.000776	0.000007	0.282846	0.000022	2.63	0.79	7.24	0.79	571	31	786	50	-0.98
18KY006-20	215	0.021197	0.000163	0.000598	0.000002	0.282849	0.000024	2.72	0.86	7.35	0.86	565	34	779	55	-0.98
18KY006-21	219	0.028385	0.000185	0.000778	0.000002	0.282831	0.000025	2.10	0.89	6.80	0.89	593	35	817	57	-0.98
18KY006-22	225	0.025271	0.000265	0.000695	0.000001	0.282861	0.000024	3.14	0.85	7.98	0.85	550	34	747	54	-0.98

18KY006-23	221	0.071799	0.000688	0.001862	0.000001	0.282775	0.000028	0.09	0.98	4.67	0.98	693	40	954	62	-0.94
18KY016-01	2466	0.009487	0.000120	0.000250	0.000001	0.281349	0.000020	-50.34	0.72	4.59	0.72	2605	27	2692	44	-0.99
18KY016-02	2420	0.016721	0.000252	0.000429	0.000003	0.281326	0.000021	-51.13	0.74	2.45	0.74	2647	28	2787	45	-0.99
18KY016-03	2420	0.033874	0.000244	0.000705	0.000003	0.281293	0.000024	-52.31	0.87	0.81	0.87	2711	33	2887	53	-0.98
18KY016-04	245	0.046494	0.000699	0.001198	0.000006	0.282840	0.000019	2.42	0.68	7.61	0.68	587	27	786	43	-0.96
18KY016-05	2437	0.005965	0.000058	0.000136	0.000001	0.281317	0.000017	-51.45	0.59	3.00	0.60	2640	22	2767	36	-1.00
18KY016-06	2447	0.016268	0.000125	0.000411	0.000001	0.281265	0.000022	-53.28	0.78	0.93	0.78	2728	29	2900	48	-0.99
18KY016-07	2503	0.006859	0.000079	0.000188	0.000001	0.281309	0.000016	-51.74	0.58	4.14	0.59	2654	22	2748	36	-0.99
18KY016-08	253	0.042683	0.000089	0.001137	0.000011	0.282823	0.000020	1.79	0.69	7.17	0.69	611	28	820	44	-0.97
18KY016-09	253	0.042719	0.000506	0.001076	0.000002	0.282891	0.000026	4.19	0.91	9.58	0.91	513	37	667	58	-0.97
18KY016-10	250	0.028780	0.001030	0.000730	0.000019	0.282787	0.000018	0.53	0.63	5.91	0.63	654	25	898	40	-0.98
18KY016-11	246	0.028871	0.000222	0.000730	0.000003	0.282850	0.000023	2.76	0.81	8.05	0.81	566	32	758	52	-0.98
18KY016-12	2449	0.013783	0.000168	0.000372	0.000001	0.281360	0.000018	-49.95	0.63	4.39	0.63	2598	24	2691	39	-0.99
18KY016-13	246	0.044325	0.000601	0.001011	0.000001	0.282797	0.000026	0.88	0.92	6.12	0.92	645	37	881	58	-0.97
18KY016-14	2486	0.012446	0.000212	0.000320	0.000002	0.281286	0.000022	-52.53	0.80	2.72	0.80	2693	30	2821	49	-0.99
18KY016-15	245	0.044285	0.000657	0.001015	0.000005	0.282787	0.000023	0.53	0.80	5.75	0.80	659	32	904	51	-0.97
18KY020-01	246.5	0.029818	0.000214	0.000813	0.000001	0.282780	0.000023	0.28	0.83	5.57	0.83	666	33	917	53	-0.98
18KY020-02	247.5	0.030075	0.000284	0.000773	0.000001	0.282766	0.000020	-0.22	0.71	5.09	0.71	685	28	948	45	-0.98
18KY020-03	248.6	0.030701	0.000441	0.000778	0.000004	0.282880	0.000025	3.81	0.89	9.14	0.89	525	35	691	57	-0.98
18KY020-04	245.8	0.018689	0.000246	0.000539	0.000003	0.282788	0.000019	0.58	0.68	5.89	0.68	649	27	896	43	-0.98
18KY020-05	247.1	0.023865	0.000117	0.000605	0.000001	0.282773	0.000019	0.05	0.66	5.38	0.66	671	26	929	42	-0.98
18KY020-06	284.3	0.048327	0.000352	0.001320	0.000014	0.282535	0.000022	-8.38	0.79	-2.38	0.79	1023	32	1449	50	-0.96
18KY020-07	245.6	0.025208	0.000280	0.000675	0.000002	0.282781	0.000024	0.33	0.85	5.62	0.85	661	34	913	54	-0.98
18KY020-08	249.9	0.037017	0.000475	0.001007	0.000004	0.282710	0.000021	-2.18	0.76	3.15	0.76	767	30	1073	48	-0.97

18KY020-09	248.6	0.020270	0.000225	0.000574	0.000001	0.282785	0.000022	0.45	0.77	5.82	0.77	655	31	902	49	-0.98
18KY020-10	249.2	0.025624	0.000369	0.000766	0.000004	0.282836	0.000018	2.27	0.63	7.62	0.63	586	25	788	40	-0.98
18KY020-11	245.0	0.020085	0.000201	0.000591	0.000002	0.282779	0.000019	0.25	0.67	5.54	0.67	663	27	917	43	-0.98
18KY020-12	252.1	0.027476	0.000510	0.000790	0.000005	0.282822	0.000020	1.75	0.71	7.16	0.71	607	28	820	45	-0.98
18KY020-13	247.6	0.030059	0.000444	0.000769	0.000003	0.282779	0.000023	0.26	0.80	5.58	0.80	666	32	917	51	-0.98
18KY020-14	245.5	0.024986	0.000571	0.000656	0.000010	0.282804	0.000017	1.13	0.60	6.42	0.60	629	24	862	38	-0.98
18KY020-15	246.9	0.021680	0.000323	0.000545	0.000004	0.282841	0.000021	2.42	0.73	7.76	0.73	576	29	777	46	-0.98
18KY020-16	244.7	0.033592	0.000648	0.000919	0.000006	0.282835	0.000024	2.23	0.85	7.46	0.85	590	34	795	54	-0.97
18KY020-17	244.5	0.019496	0.000383	0.000501	0.000005	0.282733	0.000024	-1.36	0.86	3.93	0.86	725	34	1020	55	-0.98
18KY020-18	247.2	0.037035	0.000887	0.000885	0.000027	0.282739	0.000022	-1.17	0.79	4.12	0.79	725	32	1009	50	-0.97
18KY020-19	244.8	0.022015	0.000413	0.000654	0.000004	0.282768	0.000021	-0.14	0.76	5.13	0.76	680	30	943	48	-0.98
18KY020-20	243.9	0.023652	0.000200	0.000568	0.000001	0.282767	0.000020	-0.16	0.69	5.11	0.69	679	27	944	44	-0.98

Table S4. Zircon O isotopic compositions of the standard samples and Early Triassic high-magnesium andesites in the southeastern segment of the CAOB

Sample	IP(nA)	Intensity O^{16}	O^{18}/O^{16} Mean	delta O^{18}	2SE	X position	Y position	DTFA_X	DTFA_Y	DTCA_X
18KY020-1	2.57	2931408000	0.002102698	6.54	0.21	-389	-2448	-3	18	7
18KY020-2	2.56	2911936000	0.002103456	6.92	0.23	-1034	-2456	-6	18	9
18KY020-3	2.57	2904827000	0.002104013	7.19	0.16	-1161	-2475	-8	18	10
18KY020-4	2.57	2966612000	0.002102641	6.51	0.14	-1400	-2647	-9	18	5
18KY020-5	2.57	2909013000	0.002103167	6.77	0.19	-1765	-2514	-9	18	10
18KY020-6	*2.56*	*2920462000*	*0.002098654*	*4.52*	*0.21*	*-1750*	*-2655*	*-10*	*18*	*9*
18KY020-7	2.56	2954964000	0.002103044	6.71	0.11	-2048	-2819	-14	16	8
18KY020-8	2.56	2930637000	0.002103568	6.97	0.20	-2154	-2705	-14	18	9
18KY020-9	2.55	2935348000	0.002103201	6.79	0.19	-2084	-2550	-10	19	7
18KY020-10	2.55	2903797000	0.002103690	7.03	0.21	-2218	-2822	-14	19	11
18KY020-11	2.55	2891476000	0.002103968	7.17	0.18	-2336	-2696	-13	20	10
18KY020-12	2.55	2885398000	0.002103846	7.11	0.19	-2374	-2559	-12	19	11
18KY020-13	2.53	2915175000	0.002102521	6.45	0.16	-2458	-2731	-13	19	5
18KY020-14	2.55	2915406000	0.002103746	7.06	0.19	-2525	-2581	-13	19	9
18KY020-15	2.56	2907325000	0.002103285	6.83	0.16	-2636	-2760	-15	19	10
18KY020-16	2.56	2932891000	0.002103303	6.84	0.16	-2674	-2600	-14	19	6
18KY020-17	2.56	2932295000	0.002102804	6.59	0.13	-2797	-2791	-16	19	4
18KY020-18	2.55	2943809000	0.002103678	7.03	0.17	-3166	-2798	-17	19	8
18KY020-19	2.57	2948547000	0.002102972	6.67	0.07	-3317	-2819	-17	20	4
18KY020-20	2.56	2893594000	0.002103823	7.10	0.29	-3557	-2728	-20	21	9
18KY016-1	*2.57*	*2936781000*	*0.002106383*	*8.38*	*0.13*	*168*	*-1267*	*3*	*20*	*11*
18KY016-2	*2.57*	*2912057000*	*0.002107460*	*8.91*	*0.14*	*-833*	*-1316*	*0*	*20*	*9*
18KY016-3	*2.56*	*2905146000*	*0.002105003*	*7.69*	*0.19*	*-1748*	*-1513*	*-6*	*19*	*11*

18KY016-4	2.56	2905116000	0.002100622	5.50	0.23	-2225	-1629	-7	20	10
18KY016-5	2.56	2898694000	0.002109453	9.91	0.20	-2290	-1749	-8	20	10
18KY016-6	2.56	2908870000	0.002106986	8.68	0.18	-2441	-1766	-8	20	8
18KY016-7	2.55	2924299000	0.002107213	8.79	0.22	-2891	-1556	-10	20	8
18KY016-8	2.55	2893578000	0.002099951	5.17	0.37	-2764	-1795	-10	20	10
18KY016-10	2.62	3002229000	0.002099305	4.85	0.21	-3494	-1762	-15	21	9
18KY016-11	2.62	3030037000	0.002100104	5.24	0.16	-3674	-1911	-15	21	6
18KY016-12	2.63	3003260000	0.002104393	7.38	0.19	-3709	-1802	-15	22	9
18KY016-13	2.61	2979431000	0.002099865	5.13	0.16	-4124	-1709	-16	22	5
18KY016-14	2.62	3015088000	0.002104711	7.54	0.23	-3854	-1816	-16	21	3
18KY016-15	2.61	2975751000	0.002101118	5.75	0.27	-4299	-1912	-22	22	13
18KY018-1	2.61	2956762000	0.002102820	6.60	0.15	-1899	129	1	20	12
18KY018-2	2.56	2971279000	0.002101754	6.07	0.13	-2074	245	2	20	6
18KY018-3	2.59	2980945000	0.002101654	6.02	0.15	-2330	233	2	21	5
18KY018-4	2.58	2955526000	0.002104851	7.61	0.22	-3650	-143	-6	21	7
18KY018-5	2.57	2937095000	0.002105367	7.87	0.27	-3734	42	-7	19	7
18KY018-6	2.57	2906395000	0.002104687	7.53	0.26	-3865	-71	-7	20	9
18KY018-7	2.57	2945353000	0.002103988	7.18	0.16	-3968	-106	-8	20	9
18KY018-8	2.58	2931595000	0.002101364	5.87	0.26	-4189	-120	-9	20	9
18KY018-9	2.56	2874839000	0.002105188	7.78	0.22	-4336	-233	-11	20	12
18KY018-10	2.54	2903911000	0.002103366	6.87	0.14	-4305	-114	-9	20	10
18KY019-1	2.58	2974566000	0.002101395	5.89	0.20	-2429	1263	5	20	4
18KY019-2	2.57	2949747000	0.002101268	5.82	0.16	-2724	1216	2	20	6
18KY019-3	2.56	2960446000	0.002102136	6.26	0.18	-2828	1073	1	19	5
18KY019-4	2.55	2967062000	0.002102824	6.60	0.13	-3005	1312	2	20	4

18KY019-5	2.56	2934093000	0.002102168	6.27	0.11	-3156	1136	0	19	7
18KY019-6	2.56	2932403000	0.002102146	6.26	0.15	-3266	1015	-2	19	9
18KY019-7	*2.55*	*2897157000*	*0.002102742*	*6.56*	*0.16*	*-3419*	*1247*	*-1*	*19*	*7*
18KY019-8	2.55	2911916000	0.002101730	6.06	0.14	-3602	1188	-4	19	8
18KY019-9	2.54	2882444000	0.002104150	7.26	0.32	-3684	1066	-5	18	8
18KY019-10	*2.54*	*2866430000*	*0.002103971*	*7.17*	*0.13*	*-3148*	*1030*	*-2*	*19*	*13*
Penglai1-1	2.58	2953924000	0.002099936	5.16	0.18	-3741	-2356	-19	22	5
Penglai1-2	2.58	2938390000	0.002100500	5.44	0.18	-3247	-2336	-17	21	10
Penglai1-3	2.57	2981010000	0.002099970	5.18	0.27	-2563	-2207	-14	19	10
Penglai1-4	2.56	2943861000	0.002099859	5.12	0.11	-2050	-2166	-9	19	7
Penglai1-5	2.55	2899111000	0.002100633	5.51	0.19	-1476	-2098	-8	18	12
Penglai1-6	2.54	2874236000	0.002101105	5.74	0.14	-874	-2028	-4	19	13
Penglai1-7	2.56	2940130000	0.002099793	5.09	0.12	-271	-2008	-2	17	9
Penglai1-8	2.56	2978402000	0.002099443	4.91	0.14	480	-1994	1	18	7
Penglai1-9	2.56	2939952000	0.002100701	5.54	0.20	998	-1994	2	19	13
Penglai1-10	2.55	3012383000	0.002099636	5.01	0.27	1716	-1949	6	19	6
Penglai1-11	2.62	3043359000	0.002099946	5.17	0.16	1045	-1954	3	18	6
Penglai1-12	2.62	2978766000	0.002100242	5.31	0.24	-2153	-2166	-10	18	10
Penglai2-1	2.62	3013945000	0.002099636	5.01	0.22	-660	638	7	21	8
Penglai2-2	2.58	2942457000	0.002100593	5.49	0.17	-989	616	4	20	13
Penglai2-3	2.57	2963896000	0.002099899	5.14	0.12	-1278	594	5	20	8
Penglai2-4	2.56	2947670000	0.002100249	5.32	0.10	-1730	611	3	20	9
Penglai2-5	2.55	2906204000	0.002100084	5.23	0.19	-2688	558	0	19	9
Penglai2-6	2.55	2970971000	0.002099846	5.12	0.09	-4001	434	-6	20	4
Qinghu-1	2.57	2897579000	0.002100817	5.60	0.15	-3842	-831	-14	21	13

Qinghu-2	2.56	2917008000	0.002100709	5.55	0.26	-3400	-735	-9	21	9
Qinghu-3	2.54	2917861000	0.002100733	5.56	0.19	-2654	-686	-6	21	10
Qinghu-4	2.56	2901104000	0.002101231	5.81	0.17	-1687	-567	-1	20	12
Qinghu-5	2.55	2896892000	0.002100634	5.51	0.17	-2138	-440	-1	22	9
Qinghu-6	2.62	3006199000	0.002100576	5.48	0.15	-2614	-482	-4	20	8
Qinghu-7	2.60	2550229000	0.002099770	5.08	0.47	-3835	-647	-10	20	-87
Qinghu-8	2.58	2945353000	0.002100663	5.52	0.23	-3460	-600	-8	20	9
Qinghu-9	2.56	2912427000	0.002100986	5.68	0.28	-3006	-718	-6	20	9
Qinghu-10	2.53	2921972000	0.002100833	5.61	0.17	-3074	-569	-5	20	7

Table.S5 Reported geochronological data for the Late Paleozoic-Early Mesozoic magmatic rocks along the Solonker-Xar Moron-Changchun-Yanji suture zone

Order	Sample	Lithology	Age(Ma)	Method	References
1	KY13-12-4	Basaltic andesite	250±4	LA-ICP-MS	Yuan et al., 2016
2	KY12-33-4	Andesite	ca.249	LA-ICP-MS	Yuan et al., 2016
3	DH002	Dacite	300±2	LA-ICP-MS	Yu et al., 2014
4	DH006	Dacite	302±2	LA-ICP-MS	Yu et al., 2014
5	DH008	Rhyolite	299±2	LA-ICP-MS	Yu et al., 2014
6	DH012	Basalt	299±2	LA-ICP-MS	Yu et al., 2014
7	DH020	Rhyolite	301±2	LA-ICP-MS	Yu et al., 2014
8	DH037	Rhyolitic tuff	300±2	LA-ICP-MS	Yu et al., 2014
9	DH041	Rhyolite	300±2	LA-ICP-MS	Yu et al., 2014
10	JH3S-1	Dacite	252.1±5.3	SHRIMP U-Pb	Li et al., 2007
11	D0832-6	Quartz diorite	241±1	LA-ICP-MS	Fu et al., 2010
12	D0849-1	Quartz diorite	240±1	LA-ICP-MS	Fu et al., 2010
13	FK04-5	Hornblende gabbro	241±6	SHRIMP U-Pb	Zhang et al., 2009
14	RZ08	Monzogranite	251±1.3	LA-ICP-MS	Liu et al., 2016a
15	RZ22	Granodiorite	235±1.3	LA-ICP-MS	Liu et al., 2016a
16	RZ28	Diorite	224±1.9	LA-ICP-MS	Liu et al., 2016a
17	DYS1	Rhyodacite	254.3±2.5	LA-ICP-MS	Song et al., 2018
18	DYS2	Rhyodacite	255.4±4.2	LA-ICP-MS	Song et al., 2018
19	SD7	Andesite	255.5±3	LA-ICP-MS	Song et al., 2018
20	XQ1	Rhyolite	254.7±2.6	LA-ICP-MS	Song et al., 2018
21	XDM1	Andesite	254±3.6	LA-ICP-MS	Song et al., 2018
22	XDC1	Basaltic lava	253±4.5	LA-ICP-MS	Song et al., 2018
23	DST1	Syenogranite	256.5±3.3	LA-ICP-MS	Song et al., 2018
24	LK12-1	Garnet monzonite	270±1	LA-ICP-MS	Cao et al., 2013

25	11LK15-1	Gabbro	260±5	LA-ICP-MS	Cao et al., 2013
26	11LK24-1	Syenogranite	262±2	LA-ICP-MS	Cao et al., 2013
27	LK24-1	Deformed granodiorite	255±2	LA-ICP-MS	Cao et al., 2013
28	LK36-1	Biotite syenogranite	259±2	LA-ICP-MS	Cao et al., 2013
29	12JL1-1	Syenogranite	260±1	LA-ICP-MS	Cao et al., 2013
30	LK37-1	Olivine gabbro	258±2	SIMS U-Pb	Cao et al., 2013
31	LK25-9	Monzogabbro	257±2	SIMS U-Pb	Cao et al., 2013
32	LK04-2	Biotite monzonite	249±1	LA-ICP-MS	Cao et al., 2013
33	12LY2-1	Biotite monzonite	247±1	LA-ICP-MS	Cao et al., 2013
34	LK16-1	Harzburgite	222±3	SIMS U-Pb	Cao et al., 2013
35	YH8-1	Gabbro	282±2	LA-ICP-MS	Cao et al., 2011
36	YH7-1	Diorite	255±3	LA-ICP-MS	Cao et al., 2011
37	FX06-18	Mafic rock	254±3	LA-ICP-MS	Zhang et al., 2012a
38	FX06-52	Mafic rock	252±2	LA-ICP-MS	Zhang et al., 2012a
39	FX06-59	Mafic rocks	257±4	LA-ICP-MS	Zhang et al., 2012a
40	FX06-21	Monzogranite	256±4	LA-ICP-MS	Zhang et al., 2012a
41	12JL1-1	Biotite monzogranite	260±1	LA-ICP-MS	Wang et al., 2015
42	13JH1-1	Quartz monzonite	252±1	LA-ICP-MS	Wang et al., 2015
43	13JH3-1	Hornblende gabbro	252±1	LA-ICP-MS	Wang et al., 2015
44	JK13-1	Mylonitized monzogranite	252±1	LA-ICP-MS	Wang et al., 2015
45	13YB3-2	Quartz monzonite	249±1	LA-ICP-MS	Wang et al., 2015
46	13JH28-1	Mylonitized monzogranite	245±1	LA-ICP-MS	Wang et al., 2015
47	11JJH4-1	Gabbro-diorite	256±2	LA-ICP-MS	Wang et al., 2013a
48	JK5-1	Amphibole gabbro	246±1	LA-ICP-MS	Wang et al., 2013a
49	JK17-1	Amphibole gabbro	263±1	LA-ICP-MS	Wang et al., 2013a
50	FK51	Granodiorite	284±3	SHRIMP U-Pb	Zhang et al., 2005b

51	FK53	Granodiorite	265±4	SHRIMP U-Pb	Zhang et al., 2005b
52	FK53	Hornblende	256	$^{40}Ar/^{39}Ar$	Zhang et al., 2005a
53	FK51-1	Biotite	262	$^{40}Ar/^{39}Ar$	Zhang et al., 2005a
54	FK04-19	Monzodiorite	261±2	SHRIMP U-Pb	Zhang et al., 2010
55	FK06-39	Quartz monzonite	248±2	LA–ICP–MS	Zhang et al., 2010
56	FK04-24	Granite	249±2	LA–ICP–MS	Zhang et al., 2010
57	DR40	Dacite	267±3	SHRIMP U-Pb	Liu et al., 2016b
58	12SP7	Monzogranite	396±2	LA–ICP–MS	Pei et al., 2016
59	11LK02-1	Rhyolitic tuff	410±2	LA-ICP-MS	Pei et al., 2016
60	14YT18-1	Rhyolitic tuff	403±3	LA-ICP-MS	Pei et al., 2016
61	CK85	Deformed diorite	359.4±3.5	LA–ICP–MS	Gu et al., 2018
62	CK70	Deformed granodiorite	259.1±3.1	LA–ICP–MS	Gu et al., 2018
63	CK17	Deformed granite	252.3±3.9	LA–ICP–MS	Gu et al., 2018
64	CK34	Deformed granite	367.7±7.7	LA–ICP–MS	Gu et al., 2018
65	CK07	Deformed granite	350.1±3.3	LA–ICP–MS	Gu et al., 2018
66	CK09	Deformed granite	257.5±4.0	LA–ICP–MS	Gu et al., 2018
67	CK18	Weakly deformed granite	256.6±2.8	LA–ICP–MS	Gu et al., 2018
68	CK30	Weakly deformed granite	251.5±4.1	LA–ICP–MS	Gu et al., 2018
69	CK66	Migmatized granodiorite	250.5±2.9	LA–ICP–MS	Gu et al., 2018
70	CK91	Migmatized diorite	260.8±3.8	LA–ICP–MS	Gu et al., 2018
71		Rhyolite	250±5	SHRIMP U-Pb	Chen et al., 2006
72	YY025	Granite	257±3	LA-ICP-MS	Gu et al., 2016
73	11LK19-1	Basaltic andesite	342±6	LA-ICP-MS	Wang et al., 2013b
74	11LK20-1	Rhyolite	347±5	LA-ICP-MS	Wang et al., 2013b
75		Tonalite	249±6	LA-ICP-MS	Yang et al., 2017
76		Monzogranite	248±5	LA-ICP-MS	Yang et al., 2017

77		Diorite	245±3	LA-ICP-MS	Yang et al., 2017
78		Tonalite	245±4	LA-ICP-MS	Yang et al., 2017
79	SMZG-1	Granodiorite	263 ± 1	LA-ICP-MS	Liu et al., 2010
80	SMZM-1	Gabbro	262 ± 1	LA-ICP-MS	Liu et al., 2010
81	YZ02-12-3	Tonalite	285±9	LA-ICP-MS	Zhang et al., 2004
82	YZ02-22-2	Monzogranite	245±6	LA-ICP-MS	Zhang et al., 2004
83	YZ02-25-2	Monzogranite	245±3	LA-ICP-MS	Zhang et al., 2004
84	YZ02-27-2	Monzogranite	248±2	LA-ICP-MS	Zhang et al., 2004
85	YZ02-2	Monzogranite	249±4	LA-ICP-MS	Zhang et al., 2004
86	YZ02-40	Granodiorite	246 ± 3	LA-ICP-MS	Zhang et al., 2004
87	YZ02-49	Quartz diorite	251 ± 2	LA-ICP-MS	Zhang et al., 2004
88	DY143-2	Monzogranite	252±2	LA-ICPMS	Wu et al., 2011
89	MG-28	Granodiorite	243±5	SHRIMP U-Pb	Wu et al., 2011
90	MG-64	Monzogranite	242±7	SHRIMP U-Pb	Wu et al., 2011
91	MG-103	Granodiorite	243±5	SHRIMP U-Pb	Wu et al., 2011
92	MG-143	Monzogranite	261±20	SHRIMP U-Pb	Wu et al., 2011
93	MG-119	Monzogranite	254±8	SHRIMP U-Pb	Wu et al., 2011
94	DY123-4	alkali feldspar granite	251±2	LA-ICP-MS	Wu et al., 2011
95	DY124-2	Alkali feldspar granite	260 ± 3	LA-ICP-MS	Wu et al., 2011
96	DY126-2	Syenogranite	259 ± 3	LA-ICP-MS	Wu et al., 2011
97	FW00-121	Quartz syenite	264 ± 5	SHRIMP U-Pb	Wu et al., 2011
98	FW00-34	Diorite	247±1	SHRIMP U-Pb	Wu et al., 2011
99	FW00-45	Quartz diorite	260±2	LA-ICP-MS	Wu et al., 2011
100	FW00-104	Alkali feldspar granite	253 ± 2	LA-ICP-MS	Wu et al., 2011
101	FW00-110	Monzogranite	247 ± 1	TIMS U-Pb	Wu et al., 2011
102	FW00-122	Monzogranite	240 ± 2	LA-ICP-MS	Wu et al., 2011

103	FW02-191	Alkali feldspar granite	253±2	LA-ICP-MS	Wu et al., 2011
104	FW02-194	Quartz diorite	253±2	LA-ICP-MS	Wu et al., 2011
105	YB03-188	Monzogranite	266 ± 3	LA-ICP-MS	Wu et al., 2011
106	YB03-238	Diorite	257 ± 5	LA-ICP-MS	Wu et al., 2011
107	YB03-253	Tonalite	277 ± 3	LA-ICP-MS	Wu et al., 2011
108	FW00-50	Syenite	229±3	LA-ICP-MS	Wu et al., 2011
109	07YB23	Gabbro	229±2	LA-ICP-MS	Wu et al., 2011
110	07YB04	Syenite	228±2	LA-ICP-MS	Wu et al., 2011
111	YB03-127	Monzogranite	227±4	LA-ICP-MS	Wu et al., 2011
112	07YB36	Syenite	225±2	LA-ICP-MS	Wu et al., 2011
113	YZ02-43	Quartz diorite	220±2	LA-ICP-MS	Wu et al., 2011
114	YB03-201	Syenogranite	218±2	LA-ICP-MS	Wu et al., 2011
115	99SW109	Gabbro	216±5	SHRIMP U-Pb	Wu et al., 2011
116	YB03-77	Syenogranite	216±4	LA-ICP-MS	Wu et al., 2011
117	FW00-86	Monzogranite	215±5	TIMS U-Pb	Wu et al., 2011
118	JH4-1	Rhyolite	279±3	LA-ICP-MS	Cao et al., 2012
119	JK11-1	Metadacite	293±2	LA-ICP-MS	Cao et al., 2012
120	JK11-4	Rhyolite	286±2	LA-ICP-MS	Cao et al., 2012
121	YH15-1	Basaltic andesite	275±7	LA-ICP-MS	Cao et al., 2012
122	YH2-1	Basalt	250±5	LA-ICP-MS	Cao et al., 2012
123	JXNC-I-2	Gabbro	270±10	SHRIMP U-Pb	Zhao et al., 2008
124	Jxnc-595-2	Metadacite	274 ±7	SHRIMP U-Pb	Yu et al., 2008
125	XCO3- 4	Amphibolite	274± 6	LA-ICP-MS	Zhang et al., 2007
126	13CM61	Monzonite	322.9±3.4	LA-ICP-MS	Zhang S et al., 2012
127	9-51	Monzogranite	320.3 ± 3.5	LA-ICP-MS	Zhang S et al., 2012
128	9923—1	Granite	248±4	TIMS U-Pb	Sun et al., 2004

129	B4135-2	Granite	252.8±0.7	LA-ICP-MS	Shi et al., 2013
130	16YT1-7	Andesite	280±1	LA-ICP-MS	Zhou et al., 2018
131	13YT10-1	Basaltic andesite	279±1	LA-ICP-MS	Zhou et al., 2018
132	14SP12-1	Monzogranite	256±2	LA-ICP-MS	Zhou et al., 2018
133	XNC–12	Dioritic enclave	257±4	LA–ICP-MS	Ma et al., 2019
134	XNC–43	Diorite	260±6	LA–ICP-MS	Ma et al., 2019
135	XNC–57	Granodiorite	261±5	LA–ICPMS	Ma et al., 2019
136	XNC–77	Tonalite	259±7	LA–ICP-MS	Ma et al., 2019
137	XNC–98	Gabbroic enclave	257±6	LA–ICP-MS	Ma et al., 2019
138	RZ39	Gabbro-diorite	266±2	LA–ICP-MS	Liu et al., 2020
139	RZ38	Monzodiorite	260±2	LA–ICP-MS	Liu et al., 2020
140	RZ08	Monzogranite	251±1	LA–ICP-MS	Liu et al., 2020
141	CP–1	Monzogranite	274±4	TIMS U–Pb	LBGMR, 1998
142	09HCH–12	Gabbro	254±3	LA–ICP-MS	Guo et al., 2016
143	06HCH–55	Gabbro	273±2	LA–ICP-MS	Guo et al., 2016
144	09HC–26	Diorite	263±3	LA–ICP-MS	Guo et al., 2016
145	09HC–18	Gabbro	257±2	LA–ICP-MS	Guo et al., 2016
146	BJZ-3	Quartz syenite porphyry dike	218±6	SHRMP U-Pb	Miao et al.,2005
147	JEDG-4	Granodiorite dike	223±2	SHRIMP U-Pb	Miao et al.,2005
148	2859120	Granite	216±3	LA-ICP-MS	Sun et al., 2005
149	PA09-3	Monzogranite	238.2±2	LA-ICP-MS	Zhang et al., 2012b
150	FX09-1	Monzogranite	221.7±1.7	LA-ICP-MS	Zhang et al., 2012b
151	FX09-11	Granite	221.3±2.8	LA-ICP-MS	Zhang et al., 2012b
152	DSL09-4	Granodiorite	219.6±2	LA-ICP-MS	Zhang et al., 2012b
153	FX09-2	Granodiorite	218.4±1.8	LA-ICP-MS	Zhang et al., 2012b
154	BJGC-TW1	Granodiorite	248.2±1.5	LA–ICP–MS	Shi et al., 2020

155	DXLC-TW1	Granodiorite	264.6±5.9	LA–ICP–MS	Shi et al., 2020
156	QJM-TW2	Biobite granodiorite	257.7±3.1	LA–ICP–MS	Shi et al., 2020
157	HJT-TW1	Granite	248.2±1.8	LA–ICP–MS	Shi et al., 2020
158		Gabbro	224	K-Ar	Qi et al., 2003
159		Horndiorite syenite	223±1	LA-ICP-MS	Qi et al., 2003
160	75TW14	Monzogranite	236. 9 ±1. 1	LA-ICP-MS	Yan et al.,2018
161	75TW17	Monzogranite	236. 5 ± 1. 1	LA-ICP-MS	Yan et al.,2018
162	D301-TW1	Andesite	369.6 ± 2	LA-ICP-MS	Shi et al., 2021
163	EDG-TW3	Gabbro	350.1 ± 1.8	LA-ICP-MS	Shi et al., 2021
164	PM201-4-TW1	Gabbro diorite	256.8 ± 9.9	LA-ICP-MS	Shi et al., 2021
165	PM201-3-TW1	Basalt	249.8 ± 6.7	LA-ICP-MS	Shi et al., 2021
166	BJGC-TW1	Granite	248.2 ± 1.5	LA-ICP-MS	Shi et al., 2021
167	N-8	Quartz diorite	257.8±0.9	LA–ICP–MS	Guan et al., 2016
168	P4B16-2	Monzogranite	238.5±2.8	LA–ICP–MS	Guan et al., 2016
169	B5157-1	Monzogranite	243.2±1.1	LA–ICP–MS	Guan et al., 2016
170	D2344TW1	Monzogranite	283 ± 2	SHRIMP U–Pb	Shi et al., 2019
171	PM504-2-1	Syenogranite	276 ± 2	SHRIMP U–Pb	Shi et al., 2019
172	D6219TW1	Biotite granodiorite	265 ± 1	SHRIMP U–Pb	Shi et al., 2019
173	D1694TW1	Biotite granodiorite	261 ± 1	SHRIMP U–Pb	Shi et al., 2019
174	DGTW03	Granodiorite mylonite	250 ± 3	SHRIMP U–Pb	Shi et al., 2019
175	D6008TW1	Monzogranite	245 ± 2	SHRIMP U–Pb	Shi et al., 2019
176	PM603-10-1	Biotite granodiorite	241 ± 2	SHRIMP U–Pb	Shi et al., 2019
177	D2503TW1	Biotite monzogranite	227 ± 2	SHRIMP U–Pb	Shi et al., 2019
178	CP-1	Monzogranite	274 ± 4	TIMS U–Pb	LBGMR , 1996
179	YJT-1	Monzogranite	229 ± 1	TIMS U–Pb	LBGMR, 2003